INVESTIGATING THE INTERACTION BETWEEN MOUSE TRAF1 AND THE LINEAR UBIQUITIN CHAIN ASSEMBLY COMPLEX

A Thesis submitted to the Faculty of Graduate studies in partial fulfilment of the requirements for the degree of Master of Science

GRADUATE PROGRAM IN KINESIOLOGY AND HEALTH SCIENCE

YORK UNIVERSITY

TORONTO, ONTARIO

APRIL 2022

ABSTRACT

Rheumatoid Arthritis is an autoimmune disease characterized by chronic inflammation. Tumor necrosis factor receptor (TNFR)- associated factor 1 (TRAF1) has been implicated in disease development. TRAF1 is a signalling adapter downstream of TNFR and Toll-like receptors (TLR), where it plays opposing roles in the activation of nuclear factor-k-B, NF-κB. Downstream of TNFRs, TRAF1 acts as a positive regulator of NF-κB, whereas downstream of TLRs, TRAF1 acts as a negative regulator of NF-κB. TRAF1 negatively regulates NF-κB by sequestering the Linear-Ubiquitin Assembly Chain Complex (LUBAC). Recent work in the lab has identified the exact sites of interaction of human TRAF1 in both these pathways. This thesis aims to investigate and generate a mouse model to study the role of mouse TRAF1 downstream of TLRs and its interaction with LUBAC. TRAF1 truncations and mutants have been developed which will be used to confirm the exact amino acids responsible for this interaction.

ACKNOWLEDGMENTS

I would like to thank my supervisor, Dr. Ali Abdul-Sater, for giving me the opportunity to work in his lab as a master's student. I am grateful for all the knowledge and experience that I have gained working in your lab and on this project. It was with your mentorship, support, and encouragement that enabled me to grow as a student and into the researcher that I am today.

I would also like thank all my lab mates, Fatemah A, Ali A, Ali M, Amandeep A, Bipandeep D, Mark H, Mayoorey M, Mark H, Yitian T, and Safoura Z. Thank you all for your support and guidance throughout my journey. You have all made my experience working in our lab an experience I will never forget.

Lastly, I would like to thank all my family and friends for all their constant support and love. I would not have been able to complete this journey without any of you. You all push me to be the best version of myself and I appreciate each one of you. The belief you all have in me is impeccable and has always made me believe that I can achieve anything I want. I want to especially thank my mom, who has made many sacrifices and worked countless hours to make sure our dreams were never out of reach.

TABLE OF CONTENTS

LIST OF ABBREVATIONS

RA	Rheumatoid arthritis
IL-1	Interleukin-1
TNF	Tumor necrosis factor
IgG	Immunoglobulin G
CCP	Cyclic citrullinated peptide
TLR	Toll-like receptor
TNFR	Tumor necrosis factor receptor
NLR	Nucleotide-binding oligomerization domain-like receptor
IL-1R	Interleukin-1 receptor
TIR	Toll/IL-1 receptor
LRR	Leucine-rich repeats
PAMPs	Pathogen associated molecular pattern molecules
MyD88	Myeloid differentiation primary response 88
IRAK	IL-1 receptor associated kinase
TAK	Transforming growth factor β-activated kinase **
TAB	TGF- β-activated kinase
NEMO	NF-k-B essential modulator
IKK	IκB kinase
LUBAC	Linear ubiquitin chain assembly complex
Ub	Ubiquitin
Met-1	Methionine-1
HOIL-1	Heme-oxidized IRP2 ligase-1
HOIP	HOIL-1 interacting protein
SHARPIN	Shank-associated RH domain-interacting protein
UBL	Ubiquitin-like
LDD	Linear ubiquitin-chain determining domain
NZF	Np14 zinc finger
NF-κB	Nuclear factor- kappa-B
SRR	Signal responsive region **
RHD	Rel homology domain
RING	Really interesting new gene
DAMPs	Danger-associated molecular patterns
NIK	NF-κB-inducing kinase
MAPK	Mitogen-activated protein kinase
IRF	Interferon regulatory factor
TRAF	Tumor necrosis factor receptor (TNFR) associated factor
SNP	Single nucleotide polymorphism
cIAP	Cellular inhibitor of apoptosis
BIR	Baculoviral IAP repeats

1.0 LITERATURE REVIEW

1.1 Rheumatoid Arthritis (RA)

Rheumatoid Arthritis (RA) is a chronic autoimmune disease characterized by hyperplasia, cartilage and bone destruction, and autoantibody production (1, 2). It primarily affects the small articular joints of the hands, feet, elbows, and knees resulting in synovial inflammation, which is in the joint lining (3). In RA, there is an imbalance between pro-inflammatory and anti-inflammatory cytokine production and activity, where pro-inflammatory cytokines, such as IL-1 and TNF, are favoured resulting in a hyper-reactive immune response (2). Studies indicate 0.5% to 1.0% of the world population is affected by RA, majority being women (4, 5). It has been found that genetic factors contribute to 60% of the risk for RA development (5). In 2002, it was reported that the main genetic risk factor of RA is the HLA DRB1 alleles, a gene a part of the human leukocyte antigen (HLA) family, however these genes do not completely explain the genetic effect (5). Factors, other than genetics, such as environment, hormones, and infections can contribute to the development of RA (5). Previous research has focused on the arthritis factor, which is an antibody directed against the Fc region of IgG (6). It has been used as a diagnostic tool for RA. However, it is non-specific and may be present in unaffected individuals, thus it is not optimal for the detection of RA (6). In addition, there are many other assays, such as one that uses cyclic citrullinated peptide (CCP) to detect anti-CCP antibody for the detection of RA (6).

It has been suggested that early intervention offers a high clinical response rate in individuals with RA (2, 3). One intervention that is offered includes TNF-blocking agents which work to reduce inflammation and ultimately may stop disease progression (2). One of the first TNF-blocking agents includes infliximab, also known as Remicade (7). To date, clinical studies

are still ongoing targeting various inflammatory cytokines such as IL-6, IL-15, IL-17, IL-18, and granulocyte-macrophage colony-stimulating factor (GM-CSF) (2). In addition, recent research published by Sater et al. focused on rheumatoid arthritis-associated single-nucleotide polymorphisms (SNPs) in the TRAF1 gene and their role in the development of the disease (8). Thus, it is important to understand how inflammation is initiated in immune cells, in diseases like RA, after macrophages/reactor immune cells sense pathogens via receptors, such as toll-like receptors (TLRs).

1.2 Toll-like Receptors (TLRs), Linear Ubiquitin Chain Assembly Complex (LUBAC) signalling and Nuclear Factor-kappa-B (NF-κB) Activation

The immune system is the body's first line of self defense against invading microorganisms and foreign pathogens. Innate and adaptive immunity are the two arms of the immune system that are involved in the immune response (9). TLRs, TNF-Rs, nucleotide-binding oligomerization domain-like receptors (NLRs), and interleukin-1 (IL1-R) all play a key role in the regulation of innate immunity (10). Essentially, these receptors converge at the IKK complex ultimately leading to the activation of NF-ϰB (10). Not only are TLRs essential to the activation of innate immunity, they are key receptors for the development of antigen-specific adaptive immune responses (9, 11). There are 10 members of the human TLR family, all of which have individual roles in recognizing specific microbial components (9). In addition, TLRs are membrane bound and members of the IL-1 receptor family, thus they share a very similar cytoplasmic domain termed the Toll/IL-1 receptor (TIR) domain (9). However, the extracellular domains of TLRs differ from IL-1 receptors as they contain leucine-rich repeat (LRR) motifs (12). These LRRs are responsible for the recognition of a variety of pathogen associated molecular pattern molecules (PAMPs) (12). Upon recognition of microbial components, TLR dimerization results in the activation of myeloid differentiation primary response 88 protein (MyD88), a TIR-containing adaptor, which leads to

the recruitment and activation of IL-1 receptor associated kinase (IRAK) 4 and IRAK1 (12, 13). As shown in figure 1, TRAF6, an E3 ubiquitin ligase, is recruited by IRAK1/4 to catalyze K63-polyubiquitination chains to transforming growth factor β-activated kinase (TAK) 1, TGF-β-activated kinase (TAB1), TAB2, and NF-ϰB essential modulator (NEMO) for the activation of the IKK complex (13). In addition, the activation of the IKK complex also requires linear ubiquitination of NEMO by the Linear Ubiquitin Chain Assembly Complex (LUBAC) (13).

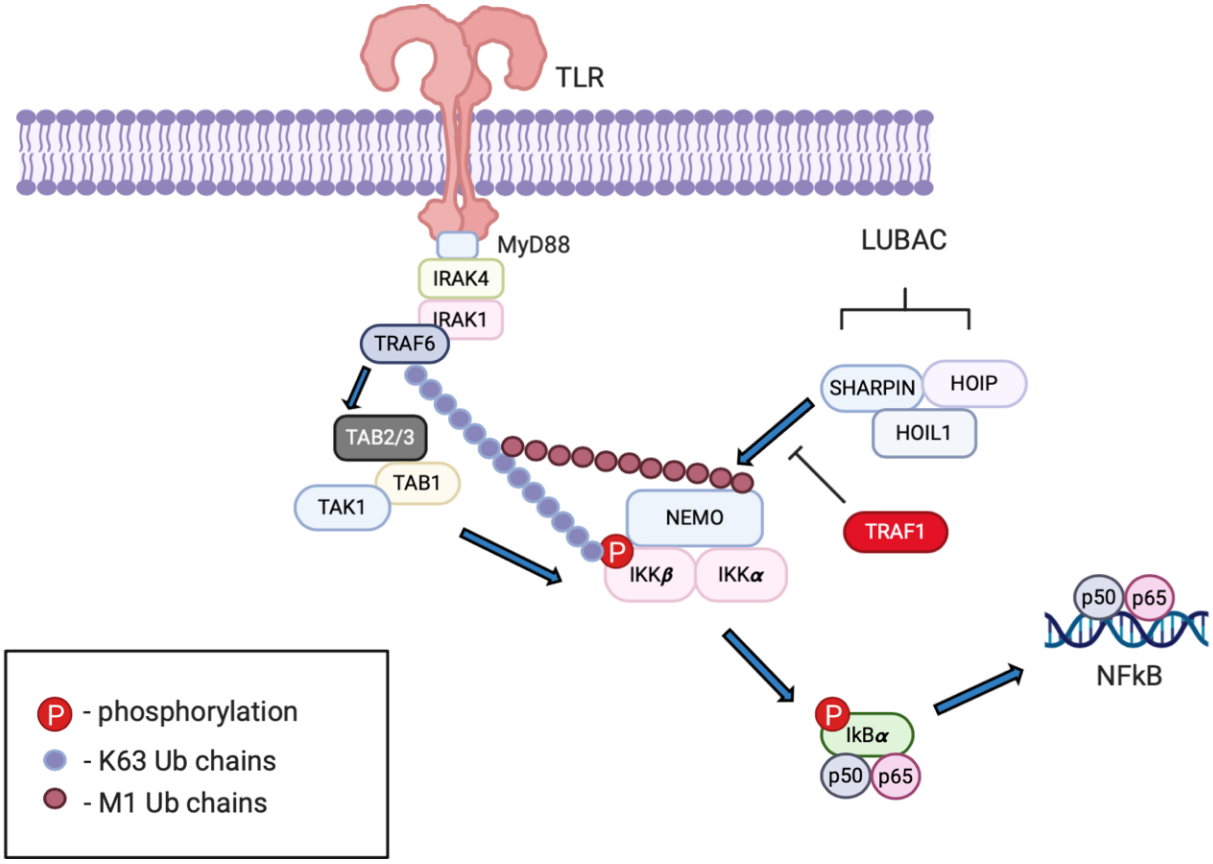

Figure 1.0 An overview of the NF-κB activation pathway downstream of TLR activation (8). Image created on BioRender.com

The activation of the IKK (IϰB kinase) complex is essential for NF-ϰB signalling as many of the diverse signalling pathways that lead to NF-ϰB activation, converge at the IKK complex

(13, 14). As shown in figure 1, IKK is a protein complex composed of three subunits, which include IKKα, IKKβ, and NEMO (IKKγ) (15). The activation of the IKK complex occurs as TRAF6 catalyzes K63-linked polyubiquitin chains to NEMO in conjunction with the linear ubiquitination of NEMO via the LUBAC complex (13). As previously mentioned, NF-κB proteins are normally sequestered by a family of inhibitory of κB (IκB) proteins in the cytoplasm characterized by the presence of ankyrin repeats that bind NF-κB and inhibit its activity (16). The IκB proteins contain an amino-terminal signal responsive region (SRR), which contain conserved serine residues that bind the IKKβ subunit (14). Thus, once activated, IKK phosphorylates IκBα, an inhibitory protein that sequesters NF-κB (17). The phosphorylation of IκBα results in its degradation in the proteasome and subsequent activation of NF-κB (14). NF-κB translocates into the nucleus where it initiates the transcription of various inflammatory cytokines and genes (15, 17, 18). In particular, NF-κB is a transcription factor vital for regulation of the innate and adaptive immune system through the expression of many immune and inflammatory genes, some of which include IL-1, IL-6, and TNFα (17). The canonical NF-κB pathway is activated by pro-inflammatory signals such as cytokines, pathogen-associated molecular patterns (PAMPs), and danger-associated molecular patterns (DAMPs) (18). This pathway relies on the proteasomal degradation of IκB proteins following phosphorylation by the IKK complex, in order to mediate the transcription of inflammatory cytokines, chemokines, and inflammasome activation (14, 18, 19). The noncanonical activation of NF-κB is NEMO-independent and primarily relies on the activity of the NF-κB-inducing kinase (NIK) (18, 19).

The LUBAC complex is an E3 ubiquitin ligase that catalyzes the addition of ubiquitin proteins to molecular scaffolds, in a linear form, which ultimately leads to NF-κB activation (20).

Ubiquitin (Ub) is a 76-residue protein involved in the regulation of protein activity, stability, and proteasome degradation through the Ub-proteasome pathway (21). The polyubiquitin chains are composed of individual ubiquitin molecules linked together through a N-terminal amino group of methionine-1 (Met 1) or a C-terminal glycine and a lysine residue in a substrate protein (21, 22). Some commonly used linkages during polyubiquitination include linear ubiquitin/Met-1 chains, K48-linked Ub chains and K63-linked Ub chains, all of which deploy specific characteristics and functions (21, 23). The LUBAC complex is comprised of 3 subunits which include the heme-oxidized IRP2 ligase-1 (HOIL-1), HOIL-1 interacting protein (HOIP), and the Shank-associated RH domain-interacting protein (SHARPIN) (20, 24). All 3 components contain ubiquitin-like (UBL) domains whereby they may bind to ubiquitin molecules or to one another (25). HOIP is the central component in the LUBAC complex and binds both HOIL-1 and SHARPIN via their respective UBL domains (25). The HOIP subunit contains a linear ubiquitin-chain determining domain (LDD) and RBR domain on its C-terminal, both of which are responsible for the synthesis of linear ubiquitin chains required for catalytic activity of LUBAC (22, 25) . In addition, all 3 components include a Np14 zinc finger (NZF) domain which also allow for the binding of Ub chains (8, 25). LUBAC mediates the activation of the IKK complex through the linear ubiquitination of NEMO with Met 1-linked chains (13). Tokunaga and Iwai investigated the effect of LUBAC on transcription and concluded the combined expression of HOIL-1-HOIP-SHARPIN induced NF-κB activity. The knockdown of the LUBAC components resulted in reduced NF-κB activities clearly indicating a direct role of LUBAC in NF-κB signalling (26). In another study, Tokunaga et al., concluded 293T cells expressing SHARPIN-HOIL-1-HOIP activated NF-κB robustly when compared to cells co-expressing HOIL-1-HOIP or SHARPIN-HOIP (24).

1.3 Tumor Necrosis Factor Receptors (TNFRs)

Tumor necrosis factor (TNF) is a superfamily of cytokines/ligands that associate with specific cell surface TNF receptors (TNFRs) (27). The subset of TNFR molecules, expressed by T cells, which include 4-1BB, CD27, and CD30, deliver signals that depend on antigen recognition (27). The TNFR family is a family of receptors involved in various signals ranging from cell survival to cell death (27, 28). In humans, there have been 19 TNF ligands and 29 TNFRs identified to date (2). TNF receptors contain an extracellular cysteine-rich domain (CRD) consisting of six cysteines and an intracellular portion that varies based on the biological activity of the receptor (28). TNFRs contain a death domain (DD) located on their intracellular portion and are responsible for initiating and activating apoptosis (28). In addition, TNF/TNFRs are involved in a variety of signalling pathways through which they initiate cellular differentiation and proliferation (28). In addition, a group of these receptors contain a TRAF-interacting motif (TIM) whereby these receptors are able to bind to TRAF proteins (29). Generally, TRAF proteins bind to these TIM domains in triplets, with multiple combinations, and relay different signals among pathways ranging from anti-inflammatory to pro-inflammatory (29).

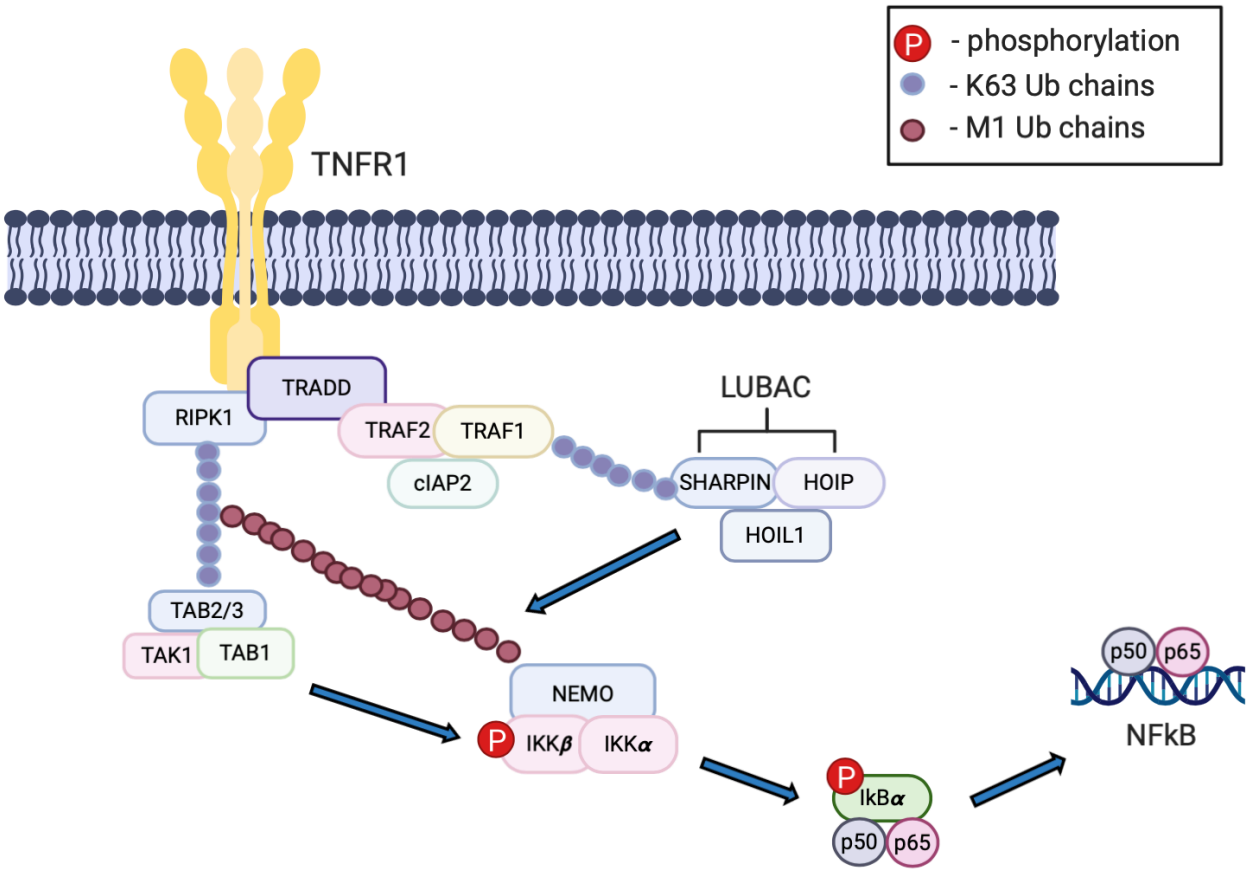

Figure 2.0 An overview of the NF-κB activation pathway downstream of TNFR receptor activation (8, 13). Image created on BioRender.com

1.4 Tumor Necrosis Factor Receptor (TNFR) Associated Factor 1 (TRAF1)

Tumor necrosis factor receptor (TNFR) associated factors (TRAFs) are a family of adaptor proteins that link TNF receptors and IL-1R/Toll receptors to signalling cascades that lead to the activation of NF-ϰB, mitogen-activated protein kinases (MAPK), and/or interferon regulatory factors (IRFs) (30, 31). Some TRAF proteins, such as TRAF 6, can function as E3 ubiquitin ligases in addition to their role as adaptor proteins (8, 31). There are six members of the TRAF family (TRAF1-TRAF6), all of which contain a N-terminal coiled-coil region (TRAF-N) and a highly conserved C-terminal Beta-sandwich domain (TRAF-C), also referred to as the meprin and TRAF-C homology (MATH) domain (13, 32, 33). The MATH domain contains minor structural

differences between TRAF proteins allowing for individual binding specificity and mediation of interactions with various receptors (32). All TRAF proteins, with the exception of TRAF1, enclose a N-terminal RING finger domain required for NF-κB activation followed by a variable number of zinc fingers (8, 20, 22).

TRAF1 has been found to serve as a positive regulator of the TNFR pathways, including TNFR1 and 4-1BB signalling pathways in T-cells (34). 4-1BB is a costimulatory receptor that, once activated, induces signals through TRAF1, ultimately leading to NF-κB activation (35). As shown in figure 2, TRAF1 binds to two TRAF2 proteins, forming a heterotrimer, which leads to the recruitment of cellular inhibitor of apoptosis (cIAP) 1 and 2 proteins (36). Inhibitor of apoptosis (IAPs) are a family of cellular proteins composed of baculoviral IAP repeating (BIR) -containing proteins, several of which bear RING domains that act as E3 ubiquitin ligases (37). The BIR domain of IAPs allow them to bind to and inhibit proteases and caspases that coordinate apoptosis, thus IAPs play an important role in the prevention of death signalling (7). As mentioned, IAPs are E3 ubiquitin ligases that lay down K63 ubiquitin chains (38). The recruitment of cIAP1/2, to the TRAF1:TRAF2 heterotrimer, results in ubiquitination of TAK and TAB2, ultimately triggering the NF-κB activation cascade (31). This trimer is more efficient in recruiting cIAPs than the TRAF2 homotrimer, thus TRAF1 plays a positive role in NF-κB induction and prevents TNF-induced apoptosis (8, 37) In addition, the E3 ligase activity of cIAP1/2, can lead to the degradation of TRAF2, however TRAF1 prevents this degradation, although the mechanism is unknown (8, 39). Ultimately, the binding of cIAP1/2 to TRAF1:TRAF2 promotes survival by transcriptionally upregulating the activity of NF-κB (40).

Recently, it has been found that TRAF1 specifically plays opposing roles, where it is a negative regulator of NF-κB activation downstream of TLR signalling and a positive regulator of NF-κB signalling downstream of TNFRs, such as 4-1BB (24). Upon TLR activation, TRAF1 binds all three subunits of the LUBAC complex and thereby reduces the linear ubiquitination of NEMO (8). The same study concluded the MATH domain of TRAF1 binds to the NZF domain of HOIP and HOIL-1 (8). In addition, TRAF1 competes with NEMO for binding with HOIP, thus in the absence of TRAF1 there is an increased recruitment of LUBAC and ubiquitination of NEMO leading to NF-κB activation (8). However, when present, TRAF1 binds to LUBAC preventing linear ubiquitination of NEMO and ultimately preventing subsequent NF-κB activation (8). In addition, under normal conditions, TRAF1 expression is inadequate for the activation of immune cells, however its expression is increased upon NF-κB activation, which acts as a negative feedback loop (8). Importantly, TRAF1 has been implicated with the development of RA (31). Genome-wide association studies first identified SNPs at the *TRAF1-C5* locus on chromosome 9 as risk factors for rheumatoid arthritis in human patients, making TRAF1 a potential target for future RA therapies (31).

Figure 3.0 Compares the identified binding region of TRAF1 in human and mouse to LUBAC.

Figure 4.0 Compares the identified binding region of TRAF1 in human and mouse cIAP2.

As discussed above, TRAF1 is a multifunctional protein whereby it plays a positive role in NF-κB regulation downstream of TNF receptors, however it also acts as a negative regulator of NF-κB downstream of TLRs. NF-κB activation is a crucial regulator of pro-inflammatory cytokines that are produced in response to infections, whereas the inhibition of NF-κB activation is crucial to prevent chronic inflammation that can be seen in diseases such as a RA (41). The dichotomous role of TRAF1 makes it difficult to appreciate its function in complex diseases, such as RA, where multiple immune cells and pathways are activated. Current work in our lab has identified the regions where human TRAF1 interact with its cIAP2 and LUBAC counterparts. Importantly, as seen in figures 3 and 4, these regions appear to be highly conserved with the mouse TRAF1. However, whether the same regions are also required for interaction between mouse TRAF1 and mouse cIAP2 and LUBAC is unknown. To study and dissect the dichotomous role of TRAF1 in disease (e.g., RA) a mouse model must be developed.

2.0 RATIONALE AND OBJECTIVES

2.1 Rationale

TRAF1 is a positive regulator of NF-ϰB downstream of lymphocyte TNFR signalling, however recent emerging evidence has showed that TRAF1 could also act simultaneously as a negative regulator of NF-ϰB downstream of TLR signalling in macrophages/monocytes. Ultimately, TRAF1 is a multifunctional adaptor protein as it plays multiple roles that depend on the cell type, pathway, and signalling receptor. As a result, the opposing roles of TRAF1 has many biological implications such as in autoimmune disease development and progression. The purpose of this thesis is to dissect and understand the role of TRAF1 in these two pathways which is essential to determine its role in diseases such as rheumatoid arthritis. Thus, the sites of interaction of human TRAF1 in both these pathways have previously been determined by our lab. I will be investigating these same regions, shown in figure 1, in mice for the same interactions with TRAF1 which will be used for future study designs. Understanding the role of TRAF1 in a complex disease, such as rheumatoid arthritis, requires an animal model to study its effects not only on the individual pathways but any consequences it may have on other biological pathways.

2.2 Objectives

1) Identify the sites of interaction between mouse TRAF1 and the individual mouse LUBAC components (HOIL-1, HOIP, and SHARPIN).
2) Identify the sites of interaction between mouse TRAF1 and mcIAP2.
3) Examine how disrupting the interactions between mouse TRAF1: LUBAC and mouse TRAF1:cIAP2 affects the signalling pathways using a functional assay.

2.3 Hypothesis

I hypothesize there will be a disruption in the signalling pathways between mouse TRAF1:cIAP2 and TRAF1: LUBAC when mutating amino acids, shown in figures 3 and 4, in the mouse cIAP2 interacting motif (CIM) and the mouse LUBAC interacting motif. Functionally, I hypothesize that TRAF1:cIAP2 mutants will block NF-κB activation downstream of 4-1BB signalling while maintaining TRAF1's ability to limit NF-κB activation downstream of TLR signalling. On the other hand, TRAF1: LUBAC mutants will cause increased NF-κB activation downstream of TLR signalling while maintaining TRAF1's ability to recruit cIAP2 and drive NF-κB activation downstream of 4-1BB signalling.

2.4 Details of Objectives

2.4.1 Objective 1: Identify the sites of interaction between mouse TRAF1 and the individual mouse LUBAC components (HOIL-1, HOIP, and SHARPIN). I will be able to achieve this by designing primers to clone mTRAF1 along with mTRAF1 deletions and mutations and mouse LUBAC into the cFlag vector. The cloned plasmids will then be overexpressed by transfection into HEK293T/17 cells. Cells will then be lysed and harvested to perform a co-immunoprecipitation to analyze protein interactions. Finally, immunoblotting will be performed to analyze the interactions between the proteins of interest.

2.4.2 Objective 2: I identify the sites of interaction between mouse TRAF1 and mcIAP2. Follows experimental design of objective 1 with mouse TRAF1 full length, deletions, truncations, and mouse cIAP2.

2.4.3 Objective 3: Examine how disrupting the interactions between mouse TRAF1: LUBAC and mouse TRAF1:cIAP2 affects the signalling pathways using a functional assay. I will achieve this

by transfecting RAW 264.7 cells with mTRAF1. Cells will be lysed and immunoblotted for the analysis of NF-κB activity.

3.0METHODS

3.1 Cell Culture

Human Embryonic Kidney cells, HEK293T/17 cells were maintained in T75 Flasks with Dulbecco's Modified Eagle Medium (DMEM) in a 37°C incubator. The DMEM contains 10% heat inactivated Fetal Bovine Serum (FBS) and 1% L-Glutamine-Penicillin-Streptomycin (GPS). The cells were passaged using 5ml of trypsin incubated at 37°C for 5 minutes, which was then followed by the addition of 5ml of DMEM media to inactivate trypsin. Centrifugation was followed at 1500 RPM for 5 minutes at 4°C and finally resuspended with desired volume of DMEM media.

3.2 Primer Design

The plasmids used in these experiments were designed using the Snap Gene program. Primers were designed to created various clones, mutations, and substitutions in the full-length mouse TRAF1 and the components of LUBAC. Primers were ordered through Integrated DNA Technologies. Table 1 below provides a list of these primers, their sequences, and ideal annealing temperature (Ta).

Table 1: List of primers used for each TRAF1 truncation/mutant and LUBAC components and their respective Ta.

Primer	Sequence (5'-3')	Ta
mTraf1ΔMath	For: ATATCTAGAACCATGG CCTCCAGCTCAGGC Rev: ATAGGATCCGGCG TGCTTGGGTGACTG	58°C
mTraf1 ΔMath+CC	For: ATATCTAGAACCATGG CCTCCAGCTCAGGC Rev: ATAGGATCCGTCTACCTCCAGGTCCCC	61°C
mTraf1ΔMath+ CC only	For: ATATCTAGAACCATGTGCTACCGGGCA Rev: ATAGGATCCGGCG TGCTTGGGTGACTG	53°C
mTraf1ΔCC	For: TCCTTTGATGGTACTTTCCTGTG Rev: GTCTACCTCCAGGTCCCC	51°C
mTraf1 V196A	For: CATTGTTGCTGCCCTCAACAAGG Rev: TTTGCAAACACACGCAGC	63°C
mTraf1 V196E	For: CATTGTTGCTGAACTCAACAAGGAAG Rev: TTTGCAAACACACGCAGC	61°C
mTraf1 E200A	For: CCTCAACAAGGCAGTGGAGGCTT Rev: ACAGCAACAATGTTTGCAAAC	63°C
mTraf1 S276A	For: GTGCCACGAGGCAGTGTGTGGCC Rev: CGCTTGGTGACATTGGTGATCTTCCAC	72°C
mTraf1 S276E	For: GTGCCACGAGGAAGTGTGTGGCC Rev: CGCTTGGTGACATTGGTG	65°C
mTraf1 R280A	For: AGTGTGTGGCGAAACTGTCAGCCTCTTC Rev: GACTCGTGGCACCGCTTG	65°C
mTraf1 R280E	For: AGTGTGTGGCGAGACTGTCAGCCTCTTCTCTCC Rev: GACTCGTGGCACCGCTTG	66°C
mHOIL-1	For: ATATCTAGAACCATGGACGAGAAGACC Rev: ATAGGTACCGTGGCAGTTTTGACAGCT	60°C
mHOIP	For: ATATCTAGAACCATGCCGGGAGACGAG Rev: ATAGGTACCCTTTCTTCTGCGGGCAAT	60°C
mSHARPIN	For: ATATCTAGAACCATGTCGCCGCCCGCC Rev: ATAGGTACCGGTGGAAGCTGCAGCAAG	60°C
cFLAG 2xmyc	For: ATAGGTACCGAGCAGAAACTCATCTCTGAAGAAGATCTG GAACAAAAGTTGATTTCAGAAGAAGATCTGTAGGAATTC ATA	60°C

	Rev: TATGAATTCCTACAGATCTTCTTCTGAAATCAACTTTTGTT CCAGATCTTCTTCAGAGATGAGTTTCTGCTCGGTACCTAT	
cFLAG 3xFlag	For: ATAGGTACCGACTACAAAGACCATGACGGTGATTATAAA GATCATGACATCGATTACAAGGATGACGATGACAAGCTA GGAATTCATA Rev: TATGAATTCCTAGCTTGTCATCGTCATCCTTGTAATCGATG TCATGATCTTTATAATCACCGTCATGGTCTTTGTAGTCGGT ACCTAT	60°C
cFLAG 2xMyc BAMH1 ECOR1	For: ATAGGATCCGAGCAGAAACTCATCTCTGAAGAAGATCTG GAACAAAAGTTGATTTCAGAAGAAGATCTGTAGGAATTC ATA Rev: TATGAATTCCTACAGATCTTCTTCTGAAATCAACTTTTGTT CCAGATCTTCTTCAGAGATGAGTTTCTGCTCGGATCCTAT	60°C

3.3 Plasmids

The various deletions and substitutions were made using mouse TRAF1 full length (TRAF-FL) as the DNA template: ΔMath, ΔMath+CC, ΔMath+CC only, ΔCC, mTraf1 S276A, mTraf1 E200A, mTraf1 V196E, mTraf1 V196A, mTraf1 R280A, mTraf1 S276E, mTraf1 R280E. These truncations and substitutions were cloned into the C-flag pcDNA3 vector from Addgene. Mouse cIAP2 and the three LUBAC subunits – HOIL-1, HOIP, and SHARPIN – were cloned from cDNA and inserted in C-flag pcDNA3 vector.

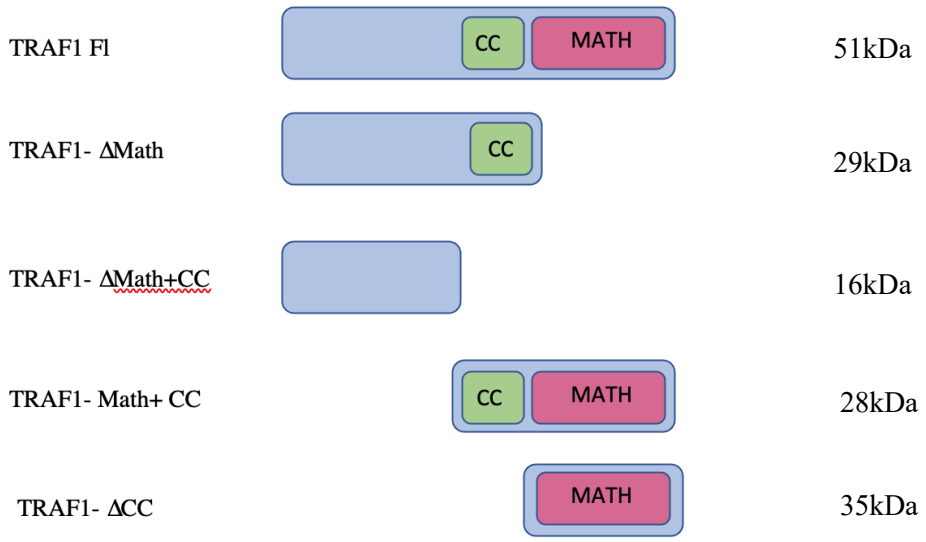

Figure 5.0 A schematic of TRAF1 Fl and the truncated domains

3.4 Site Directed Mutagenesis for TRAF1 Mutations

The Q5 Site Directed Mutagenesis Kit (NEB) was used to create the following substitutions in mouse TRAF1 - mTraf1 S276A, mTraf1 E200A, mTraf1 V196E, mTraf1 V196A, mTraf1 R280A, mTraf1 S276E, mTraf1 R280E. Primers for the various substitutions were made using the NEB Base Changer software and ordered through IDT. The protocol included in the kit that was followed.

3.4.1 PCR Amplification

To create the mouse TRAF1 mutations, the PCR product was amplified using mouse TRAF1 DNA sequence that had been cloned into c-Flag pcDNA3 as the template. Table 2.0 shows the components of the PCR reaction and table 3.0 provides the PCR protocol for the SDM.

Table 2.0 Q5 Site-Directed Mutagenesis components for PCR reaction (NEB)

Components	**25 µl Reaction**	**Final Concentration**
10 µM Forward primer	1.25 µl	0.5 µM
10 µM Reverse primer	1.25 µl	0.5 µM
Template DNA	1 µl	10 ng
Q5 Hot start high fidelity 2X Master mix	12.5 µl	1X
Nuclease-free water	9 µl	

Table 3.0 Q5 Site-Directed Mutagenesis PCR reaction conditions

Step	**Temperature**	**Time**
Initial Denaturation	98°C	30 seconds
25 cycles	98°C	10 seconds
	See table 1.0 for Ta	30 seconds
	72°C	90 seconds
Final Extension	72°C	2 minutes

3.4.2 Kinase, Ligase, and Dpnl (KLD) reaction, ligation, and transformation

Following successful PCR amplification, 1 µl of the PCR product was combined with 5 µl of the 2X KLD reaction buffer (NEB), 1 µl of the KLD enzyme mix, and 3 µl of molecular biology grade water for a total volume of 10 µl. The reaction was then incubated at room temperature for 45 minutes. 5 µl of the reaction mixture was combined with 50 µl of the competent bacteria that was provided in the kit and placed on ice for a 30-minute incubation. The mixture was then heat shocked at 42°C for 30 seconds and then placed back on ice for another 5 minutes. 950 µl of SOC broth was added to the bacteria and incubated on the orbital shaker at 37°C for 1 hour at 250RPM. Lastly, 100 µl of the mixture was spread onto agar plates with the appropriate antibiotic and placed in an incubator overnight at 37°C.

3.5 Cloning

Polymerase Chain Reaction (PCR) was used to create the mouse TRAF1 truncations and mutants to clone these plasmids into the c-Flag pcDNA3 vector. The forward primer for the following truncations: mTraf1 ΔMath, mTraf1 ΔMath+CC, and mTraf1 ΔMath+ CC only consisted of an Xba1 restriction site followed by the first 18 base pairs of the gene. The reverse primer differed, containing a BAMH1 restriction site and the last 18 complementary base pairs of the genes. For the mouse TRAF1 mutations, primers were designed using the NEBase Changer and ordered through IDT. Lastly, the forward primer for the LUBAC complex components consisted of XBa1 restriction site with the first 18 base pairs of the gene and the reverse primers consisted of the KPN1 restriction site with the last 18 complementary base pairs of the gene.

3.5.1 PCR Amplification

Primarily to clone mouse TRAF1 and its truncated derivatives as well as LUBAC into a c-Flag pcDNA3 vector, PCR product amplification was performed. Table 4.0 provides the amount of each PCR reagent used and required. Table 5.0 provides the PCR protocol conditions used upon amplification. Successfully following PCR amplification, mouse TRAF1 truncations/mutants and LUBAC were subcloned into a c-Flag pcDNA3 vector.

Table 4.0 PCR Amplification using Platinum Superfi II for mouse TRAF1 and LUBAC (ThermoFisher)

Components	**50 uL PCR Reaction**	**Final Concentration**
10µm Forward primer	2.5 µl	0.5 µM
10µm Reverse primer	2.5 µl	0.5 µM
10mM dNTPs	1 µl	200 µM
Template DNA	1 µl	10 ng
5X Superfi II Buffer	10 µl	1X
Platinum Superfi II DNA Polymerase	1 µl	1X
Nuclease free water	32 µl	

Table 5.0 PCR Conditions using Platinum Superfi II

Step	**Temperature**	**Time**
Initial Denaturation	98°C	30 seconds
25 Cycles	98°C	10 seconds
	60°C	10 seconds
	72°C	15-30 seconds/1ϰB
Final Extension	72°C	5 minutes
Hold	4°C	Infinite Hold

3.5.2 Restriction Enzyme Digestion

Subsequently upon PCR amplification, the PCR product was purified using the GenElute PCR Purification kit (Sigma) and ran on a 1% agarose gel to ensure successful amplification. These purified PCR products and the cFlag pcDNA3 vector were digested with restriction enzymes Xbal1 (NEB) and BAMH1 (NEB) (mouse TRAF1 truncations/mutations) and with Xba1 and Kpn1-HF (NEB) (LUBAC components). The reaction consisted of 43 µL of the PCR reaction, 1 µL of each corresponding restriction enzyme, 5 µL of 10X Cutsmart buffer (NEB). Simultaneously, 5 µL of cFlag pcDNA3 vector was digested using the corresponding restriction enzymes along with 38 µL of molecular biology grade water. Each reaction was incubated for 1 hour at 37°C which was followed by DNA gel electrophoresis in a 1% agarose gel. Initially, the gel was ran at 65V for 15

minutes followed by an increase to 125V for 50 minutes. The plasmids were then extracted from the gel and purified using the GenElute Gel Extraction kit (Sigma).

3.5.3 Ligation

Following purification of both the digested PCR products and vector, the PCR sequences were ligated with the vector. Using the Insilicio ligation calculation, 65ng of the vector (c-Flag pcDNA3) was ligated at a 3:1 vector: insert ratio. All reactions were composed of 4 µL of 5X Ligase Buffer (NEB), 1 µL of the T4 DNA ligase (NEB) and the corresponding amount of molecular biology grade water to a total reaction volume of 20 µL. Each reaction was incubated at room temperature for 4 hours prior to its transformation into DH5-α bacteria.

3.5.4 Transformation

DH5-α bacteria was placed on ice out of -80°C to thaw. In a snap-capped tube, 100 µl of bacteria was combined with 100ng of plasmid DNA and incubated on ice for 30 minutes. After 30 minutes, the DNA-bacteria mix was heat shocked at 42°C for 45 seconds and immediately placed back on ice for 3 minutes. After 3 minutes, 1ml of LB broth was added into the tubes under a flame and incubated in an orbital shaker at 37°C for 1 hour at 250 RPM. Agar plates containing the appropriate antibiotic were removed from 4°C and placed at room temperature to warm up. After the incubation, the solution was added to 1.5ml eppendorf tubes and centrifuged for 5 minutes at 10 000 RPM at 4°C. 600 µl of the supernatant was removed and the bacteria pellet was resuspended in the remaining solution. Lastly, 120 µl of the bacteria culture was spread onto agar plates and placed in a 37°C incubator overnight.

3.6 Plasmid Miniprep

Following the overnight incubation of the agar plates after transformation, multiple single colonies per condition were isolated and place in snap-capped tubes containing 3ml of LB broth and the appropriate antibiotic. The culture was incubated overnight in an orbital shaker at 37°C for 250 RPM. The following day, 850 µl of the overnight culture was combined with 150 µl of glycerol and placed at -80°C as a stock. The rest of the culture was used to extract the plasmid DNA using the GeneJET Plasmid Miniprep kit (ThermoFisher). Culture was centrifuged at 3000xg for 15 minutes at 4°C. The culture was resuspended with 250 µl of resuspension buffer. 250 µl of lysis solution was added and inverted 4-6 times followed by a 3-5-minute incubation. Neutralization solution was added at 350 µl and then centrifuged at 15 000xg for 5 minutes. The supernatant was transferred to a GeneJet spin column and placed through a vacuum manifold system. The column was washed twice with 500 µl of wash solution followed by centrifugation at room temperature for 1 minute. Column was eluted with 50 µl of elution buffer followed by a final centrifugation for 2 minutes. DNA concentration was measured using a nanodrop.

3.7 Plasmid Midiprep

Once it has been determined that the plasmid of interest has been successfully cloned, a midiprep was done to create higher quality and concentration of the DNA. Glycerol stocks from the previous step were used to create the starter culture in 3ml of LB broth and 3ul of the appropriate antibiotic. This culture was incubated at 37°C at 250 RPM for 6-8 hours. Afterwards, 120 µl of the day culture was added to 100 µl of LB broth and placed in the orbital shaker overnight at 37°C at 250 RPM. The following day, the PureLink Fast Low-Endotoxin Midi Plasmid Purification Kit (ThermoFisher) was used to extract the plasmids from the culture. Culture was centrifuged at 3000xg for 15 minutes at 4°C. 8mL of resuspension buffer was added to the bacterial

cell pellet for complete resuspension. Lysis buffer was added at 8mL and the tube was inverted 6 times followed by a 3-minute incubation at room temperature. 8mL of precipitation buffer was added followed by gentle inversion of tube. Lysate was filtered using the syringe filter and 8mL of binding buffer was added to filtered lysate. Lysate was added to column and filtered through the vacuum manifold system. DNA was washed with 800 µl of wash buffer 1 and 800 µl of wash buffer 2. DNA was eluted with 200 µl of elution buffer followed by final centrifugation at 10 000xg for 1 minute at room temperature. DNA concentration was measured using a nanodrop.

3.8 Plasmid Transfection into HEK293T/17 cells

Prior to the transfection of the HEK293T/17 cells, the cells were plated in 60 mm dishes at approximately $1.45x10^6$ cells per condition which led to an optimal cell confluency of 80-85% the following day. Media was removed from the cells, replaced with 5 ml of pre-warmed OPTI-MEM (Gibco), and placed at 37°C. Lipofectamine 3000 (Invitrogen) is the reagent that was used to transfect the cells with the plasmids of interest. Following the protocol listed with Lipofectamine 3000, a master-mix was made where 200 µl of OPTI-MEM per condition was added to an eppendorf tube along with the appropriate measure of lipofectamine. The DNA to Lipofectamine 3000 ratio is 1:2 as is with P3000. In addition, a second mix was made containing 200 µl of OPTI-MEM and 3 µg of the desired plasmid in separate eppendorf tubes. Separate DNA mixes were made for each plasmid. The appropriate quantity of P3000 reagent was added to the DNA mixes. The lipofectamine mix was then combined with the DNA mix, with a total volume of 400 µl, and was incubate at room temperature for 15-20 minutes. The mix was added to cells and placed in an incubator at 37°C overnight.

3.9 Lysis of HEK293T/17 cells

Transfected HEK293T/17 cells will be removed from the incubator and placed on ice. Media will be aspirated, and the cells will be washed with 3 ml of 1X Phosphate Buffered Saline (PBS). 1X PBS will be removed and 1 ml of freshly prepared co-IP lysis buffer will be added to cells. Co-IP lysis buffer contained 20 mM Tris-HCl pH8, 137 mM NaCl, 20% glycerol, 2% NP40, 2 mM EDTA, Complete Protease Inhibitor Cocktail (Roche), PhosSTOP Phosphatase Inhibitor (Sigma), 1mM DTT, and double distilled water (ddH^2O). Cells were incubated on ice with the lysis buffer for 10 minutes. Cells were scraped and added to corresponding eppendorf tubes. The cells were incubated on ice for an additional 20 minutes while vortexing every 5 minutes. After 20 minutes, cells were centrifuged at 14000 RPM at 4°C for 15 minutes. Lastly, lysates were removed, added to fresh eppendorf tubes, and placed back on ice as lysates were used to perform a co-immunoprecipitation.

3. 10 Co-Immunoprecipitation

Using the lysates extracted from the protocol above, 5 µl was removed and added to separate eppendorf tubes to be used as input. 250 µl of lysate was used to perform the co-immunoprecipitation using Protein A/G Agarose beads (ThermoFisher) and the remainder of the lysate was stored at -80°C. Desired volume of beads, 20 µl/condition, was added to a centrifuge tube. Protein beads slurry was washed with 600 µl of 1X ice cold PBS 3 times and centrifuged between each wash at 1200 rpm for 2 minutes at room temperature. Additional centrifugations between washes were performed when needed. The beads were washed with 1X Co-IP lysis buffer, centrifuged, and resuspended in the final desired volume. Beads were combined with 0.5 µg of the Flag antibody and placed on a rotator for 10 minutes at room temperature. 20 µl of Agarose beads were transferred into new centrifuge tubes and 250 µl of the corresponding lysate was added to the

centrifuge tubes containing the beads. This mix was left to incubate on the rotator at room temperature for 2 hours. Following the incubation, the beads were washed with the 1X Co-IP lysis buffer 3 times while centrifuging between washes. Then beads were washed 2 times with 1X ice cold PBS and centrifuged between washes. Finally, beads were eluted using 20 µl of 2X Laemmeli. Samples were be boiled at 100°C for 5 minutes and western blot was performed.

3.11 Immunoblotting

Initially, 10% polyacrylamide gels were made for the samples to run on. Both Co-Ip and input samples were boiled at 100°C for 5 minutes. Samples ran on the gels with the addition of Precision Plus Protein Kaleidoscope Protein Ladder (Biorad). Gels ran at 60V for 30 minutes followed by 120V for 1 hour and 20 minutes. Once gels completed their run, they were transferred onto PVDF membranes using the Trans-Blot Turbo Transfer System (Biorad) for 10 minutes at 2.5V. The membranes were be rocked for 1 hour in 5% skim milk combined in 100 ml TBST (50ml 10% TBS, 450ml double distilled water, and 250 µl tween) at room temperature. The appropriate antibody was added to the blots and incubated at 4°C overnight in 5% BSA-TBST. Table 6.0 provides a list of the primary antibodies used. The following day, membranes were washed 3x with TSBT incubating for 10 minutes for each wash. The appropriate HRP-conjugated secondary antibody was combined in 10 ml 5% skim milk in TBST was added to the membranes and incubated on the rotator for 1 hour. Membranes were washed 3x with TBST and imaged on using Clarity ECL (Biorad) on the Chemiluminescence Imager (Biorad).

Table 6.0 Primary antibodies used for Western Blot Analysis

Primary Antibody	Dilution	Company	Catalogue Number
Flag	1:1000	Sigma-Aldrich	3165
Myc	1:1000	Cell Signalling	2278

mTraf1	1:200	Santa Cruz	6253
(RNF31) HOIP	1:1000	Sigma-Aldrich	1122
(RBCK1) HOIL1	1:1000	Santa Cruz	Sc-393754

3.12 Functional Assay using RAW 264.7 cells

To determine the functional repercussions of the mouse TRAF1 mutants on NF-κB activation, RAW 264.7 cells were treated with 100ng/ml of lipopolysaccharides (LPS) at various time points. Cells were platted at $0.5x10^6$ per/well in 6-well plates. Cells were treated with LPS at 1 hour, 3-hours, 6 hours, and 24 hours timepoints. Cells were lysed following the protocol above and immunoblotted with the appropriate antibodies.

3.12.1 Cell Culture of RAW 264.7 cells

The cells that were used for the following experiment are RAW 264.7 cells. The cells were maintained in T75 flasks with DMEM in a 37°C incubator. The DMEM contains 10% heat inactivated Fetal Bovine Serum (FBS) and 1% L-Glutamine-Penicillin-Streptomycin (GPS). The cells were scrapped in 5 ml of DMEM, followed by the addition of 5 ml of DMEM. Centrifugation was followed at 1500 RPM for 5 minutes at 4°C and finally resuspended with the desired volume of DMEM.

4.0 RESULTS

4.1 Interaction between mTRAF1 and mHOIL-1

Human TRAF1 is known to interact with all three subunits of the LUBAC complex, which includes HOIL-1, SHARPIN, and HOIP (8) . More specifically, a previous student in our lab has shown that TRAF1 directly binds to LUBAC through its MATH domain at residues 281, 283, and 287. Future studies aimed at designing therapies based on targeting specific functions of TRAF1 require in vivo experiments done in mice first, where TRAF1 would be mutated to disrupt the TRAF1/cIAP2/NF-κB axis without altering the TRAF1/LUBAC/NF-κB axis, and vice versa. The first step to creating a TRAF1 mutant mouse model is to verify that mouse TRAF1 and mouse LUBAC do indeed interact with one another. While the interaction between human TRAF1 and human LUBAC components are well established, no studies have shown that TRAF1 interacts with LUBAC components in mice. Using an overexpression model in HEK293T/17 cells, the cells were transfected with full length mTRAF1 and two components of mLUBAC, both mHOIL-1 and mSHARPIN. The cloning of mouse HOIP was attempted multiple times but was unsuccessful thus it is excluded from the data. Both mHOIL-1 and mSHARPIN were tagged with a 10 AA peptide (EQKLISEEDL) c-MYC tag, allowing us to perform a co-immunoprecipitation using a flag-specific antibody that will only bind to mTRAF1 which is tagged with an 8 AA peptide (DYKDDDDK) FLAG tag. As a positive control, a FLAG-tagged mHOIL-1 and a MYC-tagged mSHARPIN were expressed together to confirm that this assay works. As negative controls, both mTRAF1 and mHOIL-1 were individually expressed with an empty pcDNA3 plasmid (c-FLAG vector) to ensure equal amounts of DNA was transfected into the cells. Following transfection, the cells were lysed, a co-immunoprecipitation was performed using a Flag-specific antibody and immunoblotted for our respective proteins.

The results show that mTRAF1 does indeed directly bind to LUBAC as seen in figure 7. This immunoprecipitation shows that mTRAF1 pulls down both mHOIL-1 and mSHARPIN. It can be noted that mTRAF1 pull down of mSHARPIN is reduced when compared to pull down of mHOIL-1. These results confirm that mTRAF1 similarly binds LUBAC as shown in the human interaction. This conclusion led us to perform a c mmunoprecipitation us mTRAF1 truncates to verify that the interaction lies in t M [d in of mTRAF1 prov n humans.

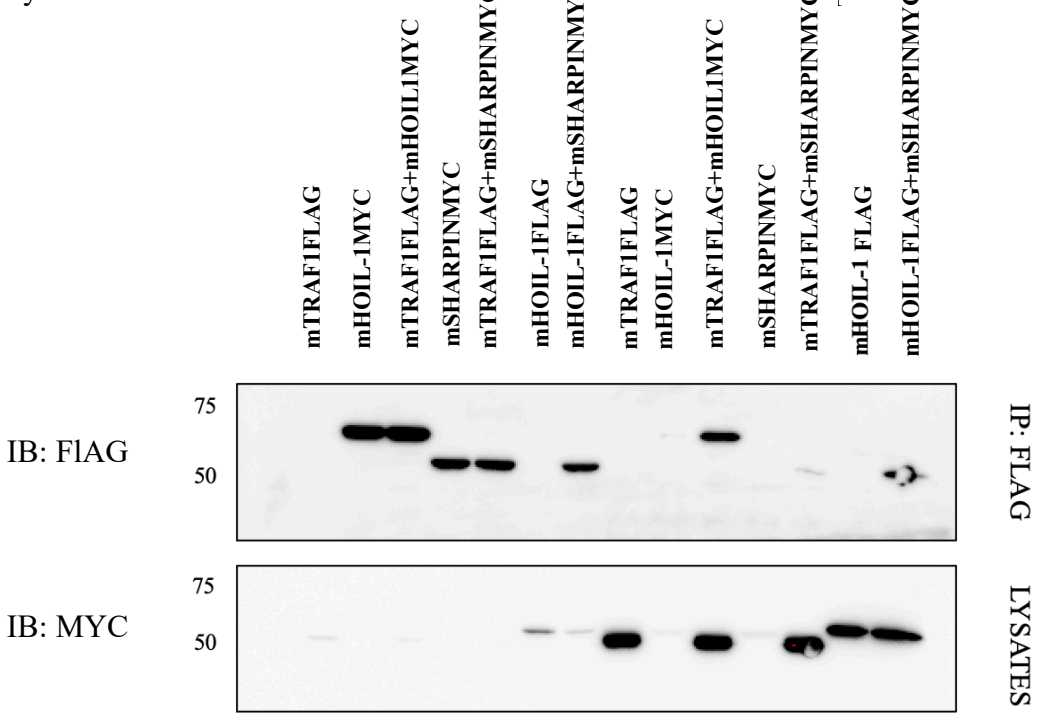

Figure 7 interaction between mTRAF1FLAG and mLUBAC components, mHOIL-1MYC and mSHARPINMYC. Co-immunoprecipitation of mTRAF1 lysates of HEK293T/17 cells, followed by immunoblotting (IB) with Myc and Flag specific antibodies and light-chain-specific anti-Rabbit-horseradish perioxidase and anti-mouse.

4.2 Effects of mTRAF1-ΔMATH, mTRAF1-ΔCC, and mTRAF1-MATH+CC on the interaction with mHOIL-1 and mSHARPIN

As previously mentioned, it has been shown that human TRAF1 binds LUBAC through its MATH domain residing between amino acids 266-412. We generated 3 different truncated

versions of mouse TRAF1 (mTRAF1), which includes mTRAF1- ΔMATH, mTRAF1 with a deleted MATH domain, mTRAF1- ΔCC, mTRAF1 with a deleted Coiled-Coil (CC) domain and mTRAF1- MATH+CC, where only the MATH and CC domain remain. Each mTRAF1 truncate was co-transfected with our protein of interest, mHOIL-1, which was also transfected on its own as a negative control. Figure 8 shows a Western Blot of a co-immunoprecipitation done using the Flag-specific antibody. The results show that mHOIL-1 interaction is abrogated with the deletion of the MATH domain when compared to full length mTRAF1. In addition, we see the interaction remains with the deletion of the Coiled-coil domain and with both the MATH and CC domain present.

In addition, we performed a second co-immunoprecipitation using another subunit of mLUBAC, mSHARPIN. The same mTRAF1 truncations from figure 8 were used and co-expressed with mSHARPIN for this experiment. As shown in figure 9, the interaction between mTRAF1 and mSHARPIN is lost with the deletion of the MATH domain when compared to full length mTRAF1. However, the interaction between these 2 proteins remains with the deletion of the CC domain. These sets of results confirm that the interaction between mouse TRAF1 and mouse LUBAC occurs in the MATH domain region of mTRAF1. For subsequent experiments aimed at identifying the interaction sites, we focused on the interaction with mouse HOIL-1 given that there is seen to be a more robust interaction with mouse TRAF1. This confirmation led us to investigate the interaction between these mTRAF1 truncates and mouse cIAP2, a key regulator protein downstream of the TNFR1 pathway.

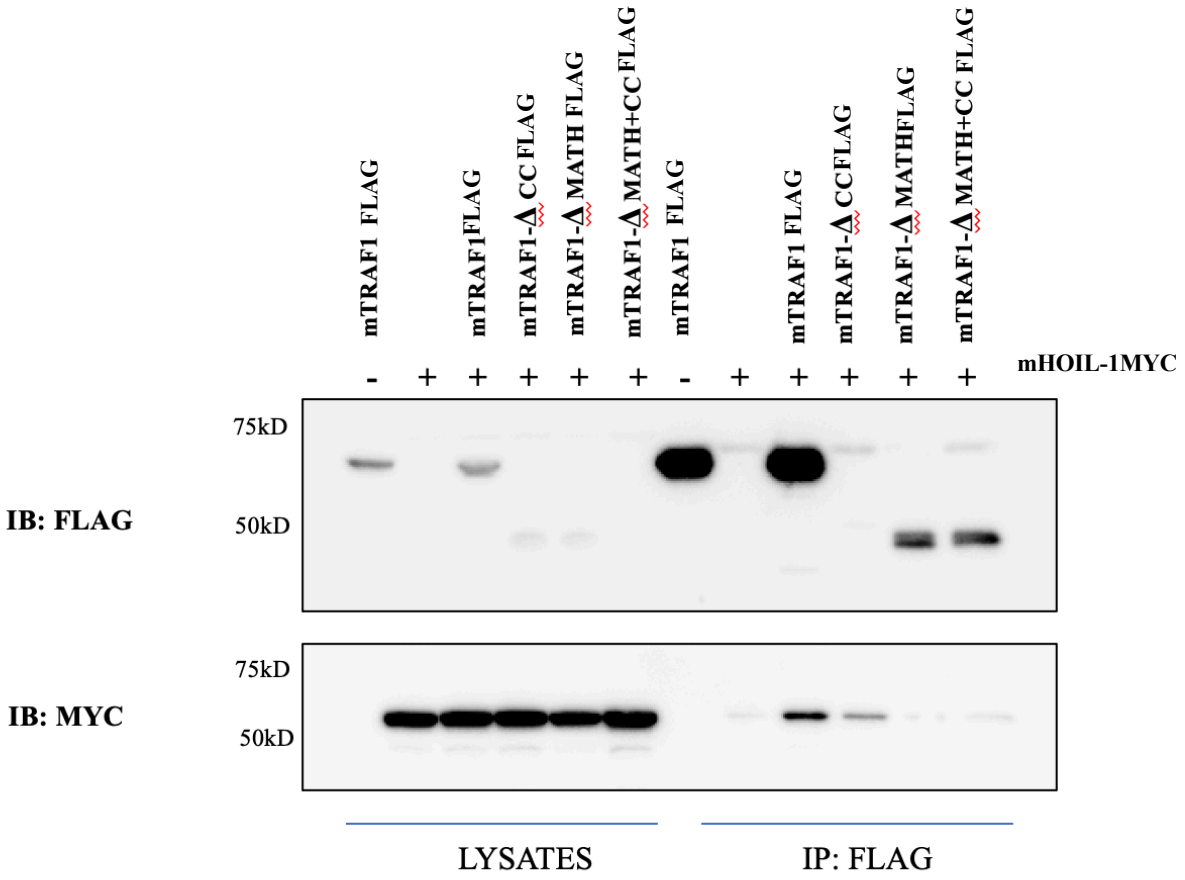

Figure 8 effects of mTRAF1FLAG deletions on mHOIL-1MYC. Co-immunoprecipitation of mTRAF1 lysates of HEK293T/17 cells, followed by immunoblotting (IB) with Myc and Flag specific antibodies and light-chain-specific anti-Rabbit- and light-chain-specific anti-mouse. This experiment was conducted three independent times.

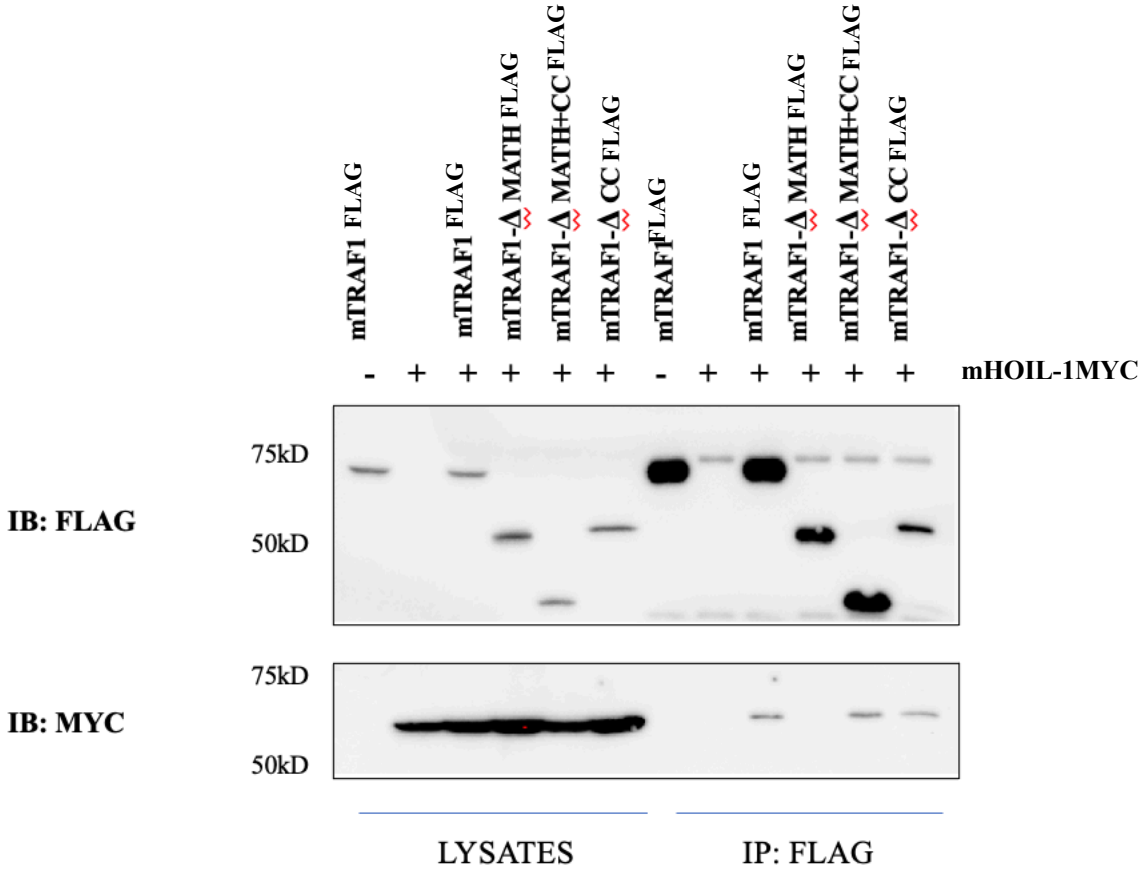

Figure 9. Effects of mTRAF1FLAG deletions on mHOIL-1MYC. Co-immunoprecipitation of mTRAF1 lysates of HEK293T/17 cells, followed by immunoblotting (IB) with Myc and Flag specific antibodies and light-chain-specific anti-Rabbit- and light-chain-specific anti-mouse.

4.3 Effects of mTRAF1-S276A, mTRAF1-R280A, mTRAF1-R280E, mTRAF1-V196A, mTRAF1-V196E, and mTRAF1-E200A on the interaction with mHOIL-1

Since we confirmed the interaction between mTRAF1 and mLUBAC does indeed occur within the MATH domain, the next step is to investigate whether the interaction occurs at residues 281 and 283. First, we translated these residues to mTRAF1 and created the corresponding mouse mutations. HEK293T/17 cells were co-transfected with mHOIL-1 and each of the mTRAF1 mutations created, mTRAF1-S276A, mTRAF1-R280A, mTRAF1-R280E, mTRAF1-V196A, mTRAF1-V196E, and mTRAF1-E200A, along with the previously mentioned mTRAF1 deletions.

A co-immunoprecipitation was performed using a TRAF1-specific antibody and immunoblotted for our respective proteins. As expected, the binding between each mTRAF1-S276A, mTRAF1-R280A, mTRAF1-R280E mutation and mHOIL-1 was still present (figure 10). This indicates that the binding sites between TRAF1 and LUBAC are not conserved between human and mouse. In addition, the mTRAF1-V196A, mTRAF1-V196E, and mTRAF1-E200A still bind to mHOIL-1, which means that the mutations made corresponding to the interaction between mTRAF1 and mcIAP2 do not interfere with the binding between mTRAF1 and mLUBAC, which is important to confirm to allow us to study the opposing roles TRAF1 plays in the canonical and noncanonical pathways. After discovering this interaction was not conserved between human and mouse, it was critical for us to investigate the conservation between the mTRAF1 and mcIAP2 binding sites found in human as well.

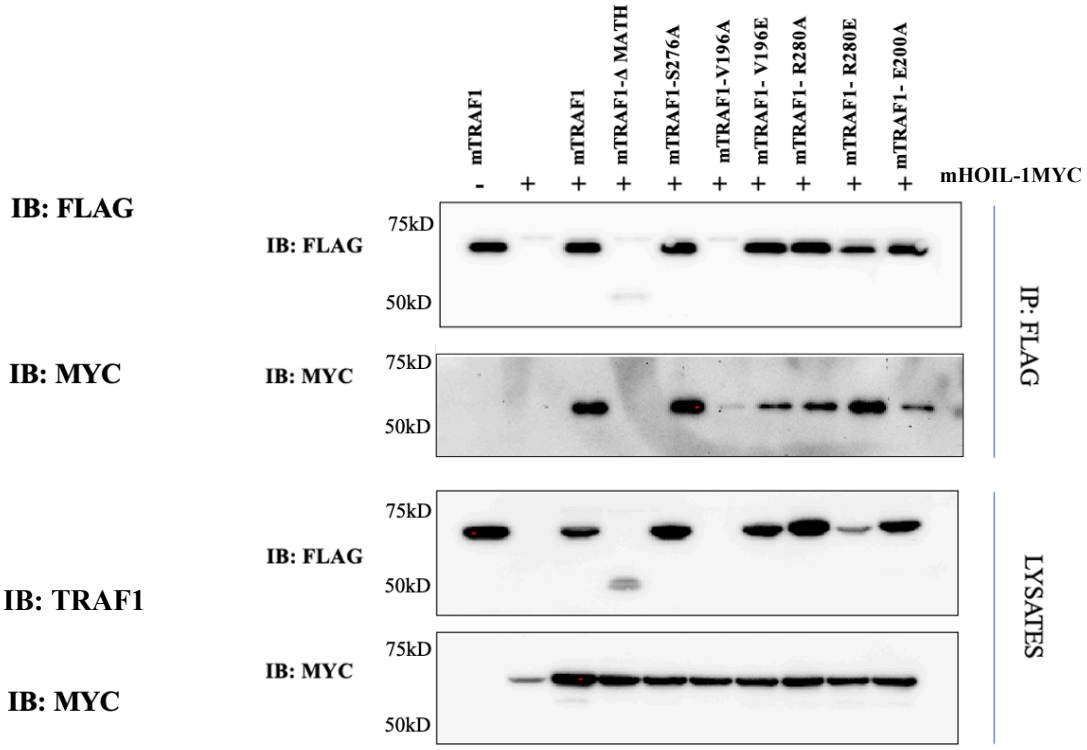

Figure 10 effects of single mTRAF1FLAG mutations on mHOIL-1MYC. Co-immunoprecipitation of mTRAF1 lysates of HEK293T/17 cells, followed by immunoblotting (IB) with Myc and Flag specific antibodies and light-chain-specific anti-Rabbit- and light-chain-specific anti-mouse. This experiment was conducted three independent times.

4.4 Investigating the interaction between mTRAF1 residues mTRAF1-1-260, mTRAF1-1-262, mTRAF1-264 and mHOIL-1

After concluding that the residues responsible for the interaction between human and mouse TRAF1-LUBAC are not conserved, we created truncations in the MATH domain to narrow where the interaction may occur in mouse. Based on the crystal structure data publicly available, we hypothesized that the interaction occurs in the loops that at the beginning of the MATH domain, therefore we deleted 2 residues of the gene at a time, mTRAF1-1-260, mTRAF1-1-262, and mTRAF1-1-264. These mutants were co-transfected with mHOIL-1, along with mTRAF1-ΔMATH, mTRAF1-ΔCC as controls, and a co-immunoprecipitation was performed using a

TRAF1 antibody. Figure 11 show that the interaction between mTRAF1 and mLUBAC is still present with the mTRAF1-1-262 and mTRAF1-1-264 truncations. However, this interaction is lost with the mTRAF1-1-260 truncation, indicating that the interaction lies between residues 260 and 262.

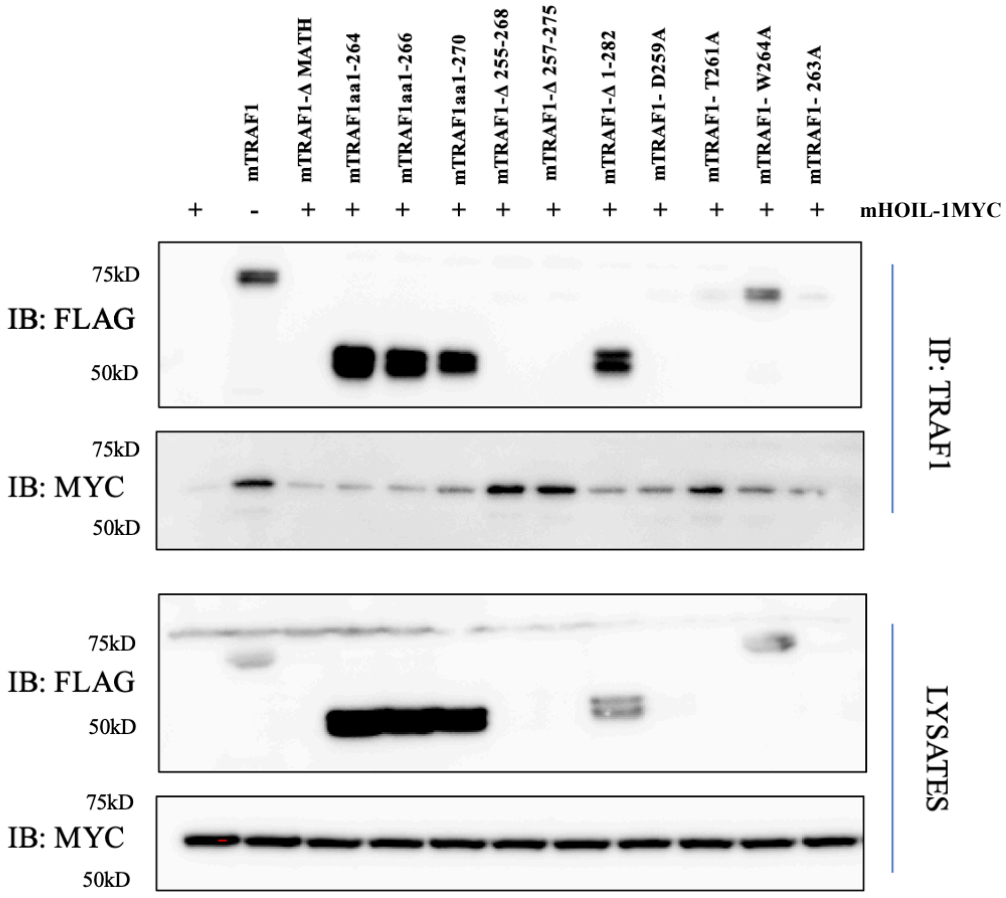

Figure 11 effects of mTRAF1FLAG mutations/truncations on mHOIL-1MYC. Co-immunoprecipitation of mTRAF1 lysates of HEK293T/17 cells, followed by immunoblotting (IB) with Myc and Flag specific antibodies and light-chain-specific anti-Rabbit- and light-chain-specific anti-mouse. This experiment was conducted three independent times.

4.5 Effect of mTRAF1 single mutations, mTRAF1-T261A and mTRAF1-W264A, on the interaction with mHOIL-1

The final step to identifying the exact sites of interaction between mTRAF1 and mLUBAC involves creating single amino acid mutations to establish the exact residue(s) responsible for this interaction. We have created mutants T261A and W264A. A mutation for residue 262 was not included due to its inability to clone. Figure 12 is a western blot of a co-immunoprecipitation performed using these mutations alongside mTRAF1-ΔMATH, which were all co-expressed with mHOIL-1. When compared to the mTRAF1-ΔMATH deletion we can see we have lost complete interaction between these single mutations and mHOIL-1. This blot clearly identifies that the interaction between mTRAF1 and mLUBAC occurs at residue 261.

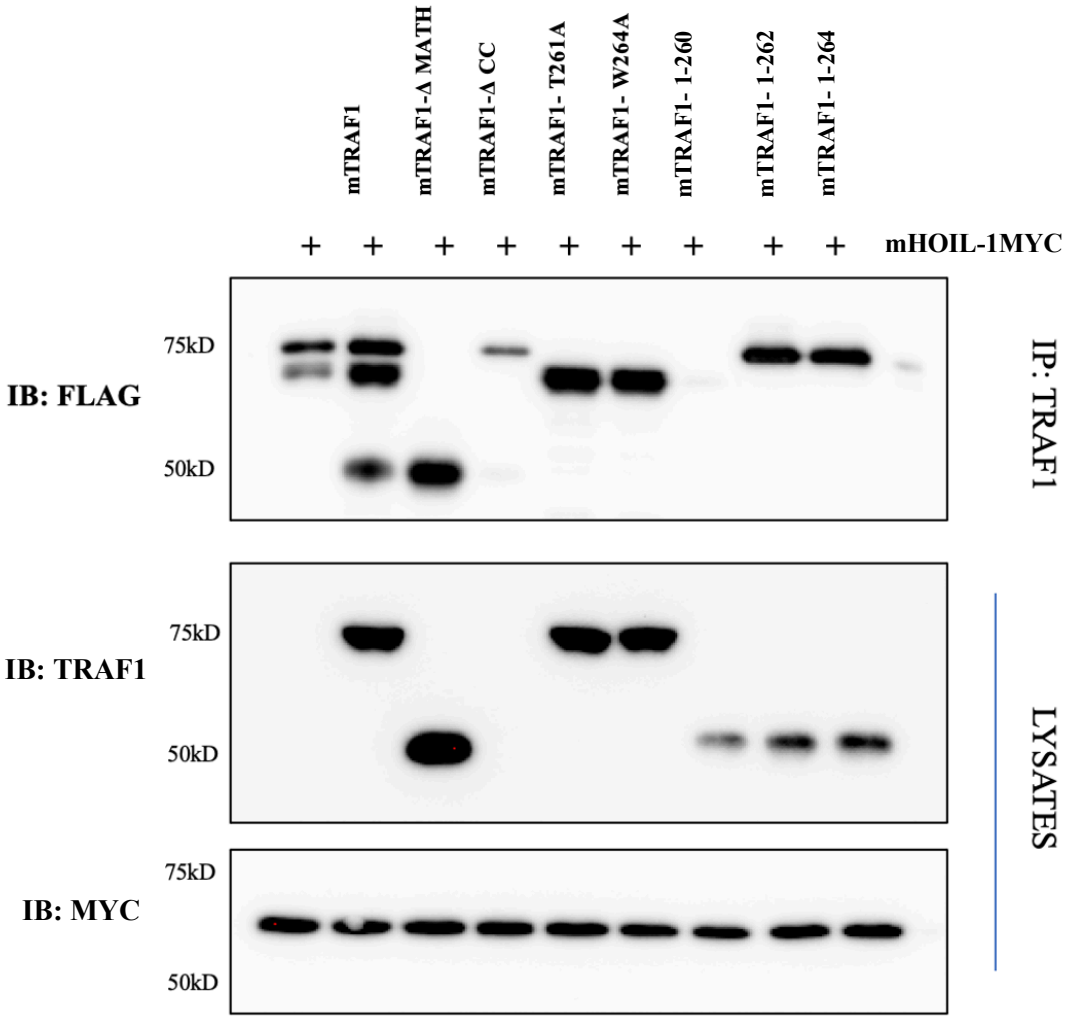

Figure 12 effects of mTRAF1FLAG truncations/mutations on mHOIL-1MYC. Co-immunoprecipitation of mTRAF1 lysates of HEK293T/17 cells, followed by immunoblotting (IB) with Myc and Flag specific antibodies and light-chain-specific anti-Rabbit- and light-chain-specific anti-mouse. This experiment was conducted three independent times.

4.6 Effects of mTRAF1-ΔMATH, mTRAF1-ΔCC, and mTRAF1-MATH+CC on the interaction with mcIAP2

As mentioned earlier, cIAP2 is an E3 ligase whose activity is essential for the upregulation of NF-κB activity (40). Ultimately, cIAP2 acts as a positive regulator of NF-κB and LUBAC acts as a negative regulator of NF-κB (13). Thus, it is important to determine the individual binding sites for these 2 proteins with TRAF1 to allow us to create a mouse model where we can separate these 2 pathways. Our lab has identified residues 203 and 207, located in the CC domain of human TRAF1, as the sites of interaction with human cIAP2. First, we need to confirm that mouse cIAP2 binds mouse TRAF1 in the CC domain as it does in the human. HEK293T/17 cells were co-transfected with our protein of interest, mcIAP2, and the mTRAF1 truncates, mTRAF1-ΔMATH, mTRAF1-ΔCC, and mTRAF1-MATH+CC. Lysates were collected, and a co-immunoprecipitation was performed using a TRAF1-specific antibody followed by immunoblotting with our respective proteins. Figure 13 shows that binding between mTRAF1-ΔMATH and mcIAP2 remains while with mTRAF1-ΔCC we can see a clear loss of interaction between the 2 proteins. Thus, it can be confirmed that the binding between mTRAF1 and mcIAP2 occurs at the CC domain of mTRAF1.

4.7 Effects of mTRAF1-V196A, mTRAF1-V196E, and mTRAF1-E200A on the interaction with mcIAP2

Even though our lab successfully identified residues 203 and 207 critical for the interaction between mTRAF1 and mcIAP2, there is reason to question whether these residues are responsible for this same interaction in mouse. We found residues 196 and 200 in mTRAF1 correspond to residues 203 and 207 respective in human TRAF1. We created these mutations and co-expressed them in HEK293T/17 cells alongside mcIAP2 and the mTRAF1 truncates as positive controls. A co-immunoprecipitation was performed using the TRAF1 specific antibody. Figure 13 shows a

western blot of this immunoprecipitation which has been immunoblotted using a FLAG and MYC antibody. The results confirm that the interaction between mcIAP2 and mTRAF1 is abolished at these residues. Thus, we confirmed that the residues responsible for this protein-protein interaction are indeed conserved between human and mouse.

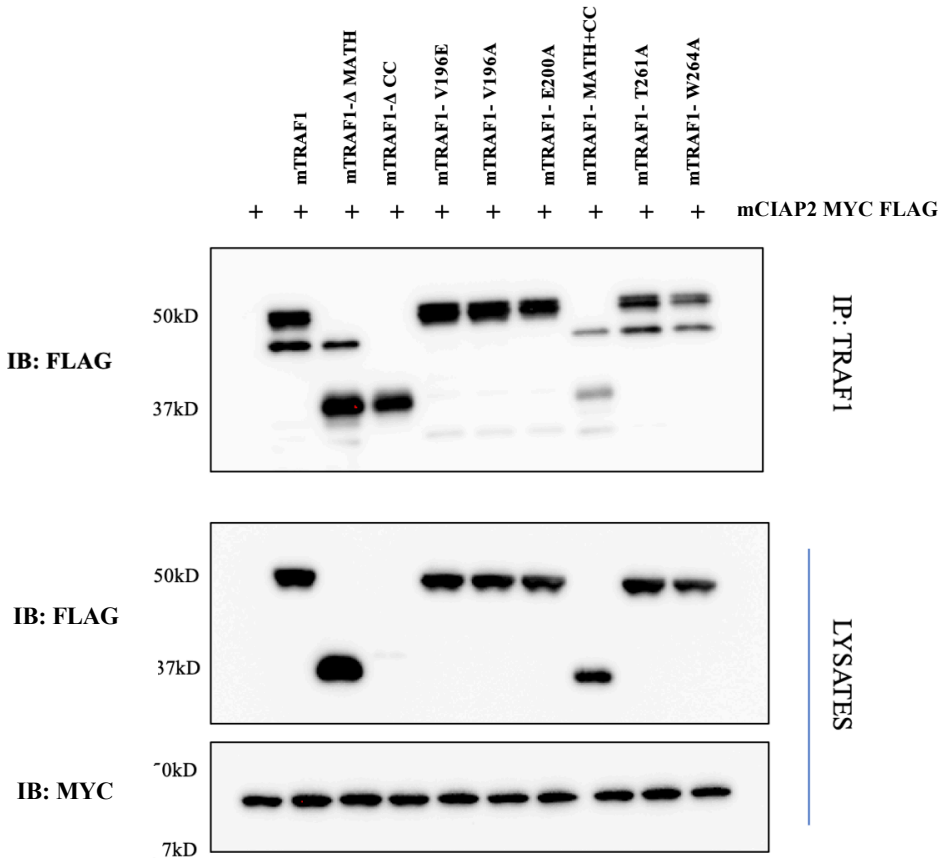

Figure 13 effects of single mTRAF1FLAG deletions/mutations on mcIAP2MYCFLAG. Co-immunoprecipitation of mTRAF1 lysates of HEK293T/17 cells, followed by immunoblotting (IB) with Myc and Flag specific antibodies and light-chain-specific anti-Rabbit- and light-chain-specific anti-mouse. This experiment was conducted three independent times.

4.8 Interaction between mTRAF1-T261A with mcIAP2

The final step of this project is to confirm that the interaction between mTRAF1 and mcIAP2 is not disrupted with the mTRAF1-T261A mutant. Again, this will allow us to create a

model where we can isolate both the canonical and non-canonical pathways of NF-ϰB and examine the dichotomous role of TRAF1 in each pathway. Once again, HEK293T/17 cells were co-transfected with mcIAP2 and mTRAF1-ΔMATH, mTRAF1-ΔCC, and mTRAF1-MATH+CC, mTRAF1-V196E, mTRAF1-V196A, mTRAF1 E200A, as controls, along with mTRAF1-T261A, and mTRAF1-W264A. The interaction between mcIAP2 and mTRAF1-T261A is still maintained and resembles the interaction between mcIAP2 and full length mTRAF1 (Figure 13). This finding concludes that mTRAF1 residue 261 is responsible for the binding between mTRAF1 and mLUBAC and does not interfere with the interaction between mcIAP2 and mTRAF1.

4.9 mTRAF1 functional assay using RAW 265.7 cells

A functional assay for these mTRAf1 mutants was attempted. Figure 14 shows LPS stimulated RAW 264.7 cells immunoblotted with TRAF1 and HOIL-1. In figure 14A, there is no detection of mTRAF1 with the stimulation of LPS. This indicates there is no production of endogenous TRAF1 in this mouse cell line. Figure 14B shows the immunoblotting with the HOIL-1 antibody. There is clear production of endogenous mHOIL-1 with LPS stimulation at each timepoint. Lastly, Figure 14C shows immunoblotting with the HOIP antibody and there is clear stimulation of HOIP in this mouse cell line. This prompted us to believe this is a potential assay where we can introduce the mouse TRAF1 assay. However, due to the poor ability of cell transfection efficiency of this mouse cell line and due to COVID, advancements for this assay were discontinued.

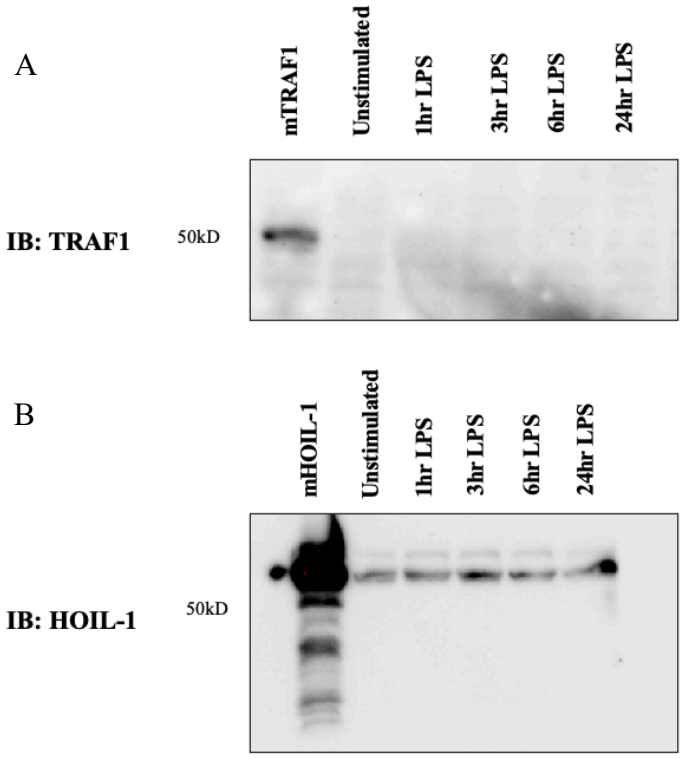

Figure 14 Effects of LPS stimulations in Raw 264.7 cells at various time points. Cell lysates of Raw 264.7 cells stimulated with 100ng/ml of LPS at 0 hr, 1 hr, 3hr, 6 hr, and 24 hr. Immunoblotting with TRAF1 and HOIL-1 specific antibodies and light-chain-specific anti-Rabbit- and light-chain-specific anti-mouse.

5.0 DISCUSSION

TRAF1 is a multifunctional protein as it plays various roles depending on the cell type, signalling pathway, and receptor involved (8, 13). Specifically, in innate immune cells, such as monocytes/macrophages, TRAF1 reduces inflammation by inhibiting NF-κB activation (4). By associating with all 3 LUBAC components, TRAF1 prevents the linear ubiquitination of NEMO implicating TRAF1 as a negative regulator of NF-κB (5, 9). In contrast, TRAF1 acts as a positive regulator of NF-κB in lymphocytes and other adaptive immune cells (4). It forms a heterotrimer with 2 TRAF2 proteins leading to the recruit of cIAP2 ultimately triggering the NF-κB activation cascade (5, 9, 31). This dichotomous role of TRAF1, as an adapter protein, is essential for the function of the immune system as it is evidently a key regulator of inflammatory genes. NF-κB is the master regulator of the immune response and activates numerous discrete cytokines and proteins essential to fight foreign pathogens (17, 18).

Dysfunction of these pathways can lead to the development of various autoimmune diseases such as rheumatoid arthritis, multiple sclerosis, and systemic lupus erythematosus (42). In particular, RA is a multidimensional disease that affects both the innate and adaptive arms of the immune system. We specifically investigated the roles and implications of TRAF1 in the development of RA. Due to the complexity of its roles, broadly targeting TRAF1 would result in increased inflammation from monocytes and, at the same time, decreased lymphocyte survival. Thus, indiscriminately blocking or enhancing TRAF1 activity is not an effective strategy to decipher its role in these pathways.

Instead, our lab proposed the distinct roles of TRAF1 should be isolated between the innate and adaptive immune systems. Our lab has successfully identified that the interaction between human TRAF1: LUBAC occurs at residues histidine 281 and serine 283 and human TRAF1:

cIAP2 occurs at residues valine 203 and glutamic acid 207. With advice from a structural biologist, each of these residues were mutated into an alanine. The next step to this strategy was to translate these mutations into mouse to create a functional model that would allow us to study the singular effect of TRAF1 in each pathway. This project specifically focused on confirming that these human interactions between TRAF1: LUBAC and cIAP2, respectively, are conserved within mouse.

We generated TRAF1 truncations in which we deleted the MATH and CC domain both exclusively and collectively. Using co-immunoprecipitations, we confirmed that the mTRAF1 interaction between LUBAC occurs within the MATH domain and cIAP2 occurs within the CC domain as seen in human (see figures 9 and 11). Next, we translated and generated the single amino acid mutations that were found to be responsible in humans for the interaction between TRAF1 and these 2 proteins in mouse. It was confirmed that the mTRAF1: mcIAP2 interaction is conserved in mouse, binding at valine 196 and glutamic acid 200. However, we found that the mTRAF1: mLUBAC sites of interaction did not translate between human and mouse (see figure 12).

Thus, we created truncations in the MATH domain of mTRAF1 to determine the site(s) of interaction between mTRAF1: mLUBAC. We established that the interaction between mTRAF: mLUBAC occurred at the origin of the MATH domain. Ultimately, using co-immunoprecipitations performed between mHOIL-1 and a multitude of single amnio acid mutations created in mTRAF1, we demonstrated that the interaction between mTRAF1: mLUBAC occurs at residues threonine 261 and tryptophan 264 (see figure 16). Figure 18 compares these identified regions in mouse to human. It can be clearly seen that these regions are highly conserved between the two species.

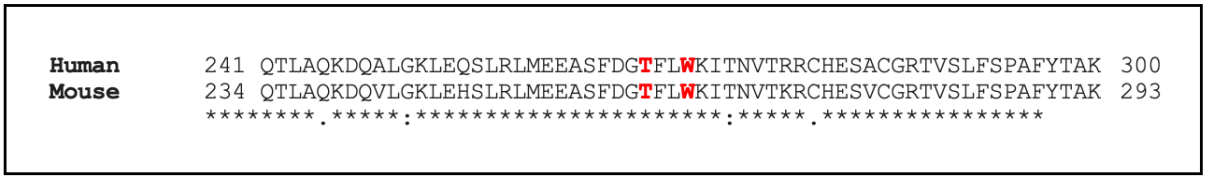

Figure 18 Compares the newly identified binding regions in TRAF1 responsible for the interaction with LUBAC in human and mouse

Although we were able to determine and confirm the exact loci responsible for the interactions between mTRAF1 in both, innate and adaptive immune cell, we were unable to create a functional assay that would verify the effects of these mutants. The objective of this functional assay was to verify that these mTRAF1 mutants nullify its role in, either increasing or decreasing, NF-κB activation. Initially, we used a Nano-Glo Luciferase Assay System (Promega) to overexpress mHOIL-1, mSHARPIN, and both together in HEK293T/17 NF-κB-Luciferase cells along with a Renilla luciferase. It has been shown that both these components drive the activation of NF-κB. For this assay, we were measuring bioluminescence in the cells as it directly corresponds with the effect mHOIL-1 and mSHARPIN have on the expression of NF-κB. We were expecting to see an increased bioluminescence when compared to our control with the overexpression of these proteins, however we failed to do so due to inconsistencies with the assay.

We, next, stimulated RAW 264.7 cells with LPS (100ng/ml) at various time points (1hr, 3hr, 6 hr, 24hr) to examine endogenous levels of mTRAF1 and mLUBAC. We concluded RAW 264.7 cells do not have endogenous levels of mTRAF1 or produce undetectable amounts. We did, however, detect endogenous levels of mHOIL-1. In theory, this system allows us to introduce mTRAF1, full length and our mutants, into these cells to validate the effects we believe these

mutations would have. However, RAW 264.7 cells have very poor transfection efficiency thus we were unable to introduce these plasmids into these cells.

Essentially with a functional assay, we want to ensure mTRAF1-V196A, mTRAF1-V196E, and mTRAF1-E200A can decrease NF-κB activation without hindering the interaction between mTRAF1: mLUBAC. In contrast, we hope to confirm mTRAF1-T261A and mTRAF1-W264A can increase NF-κB activation without affecting the interaction between mTRAF1: mCIAP2. Figure 21 illustrates a clear schematic of TRAF1s roles downstream of TLRs and TNFRs.

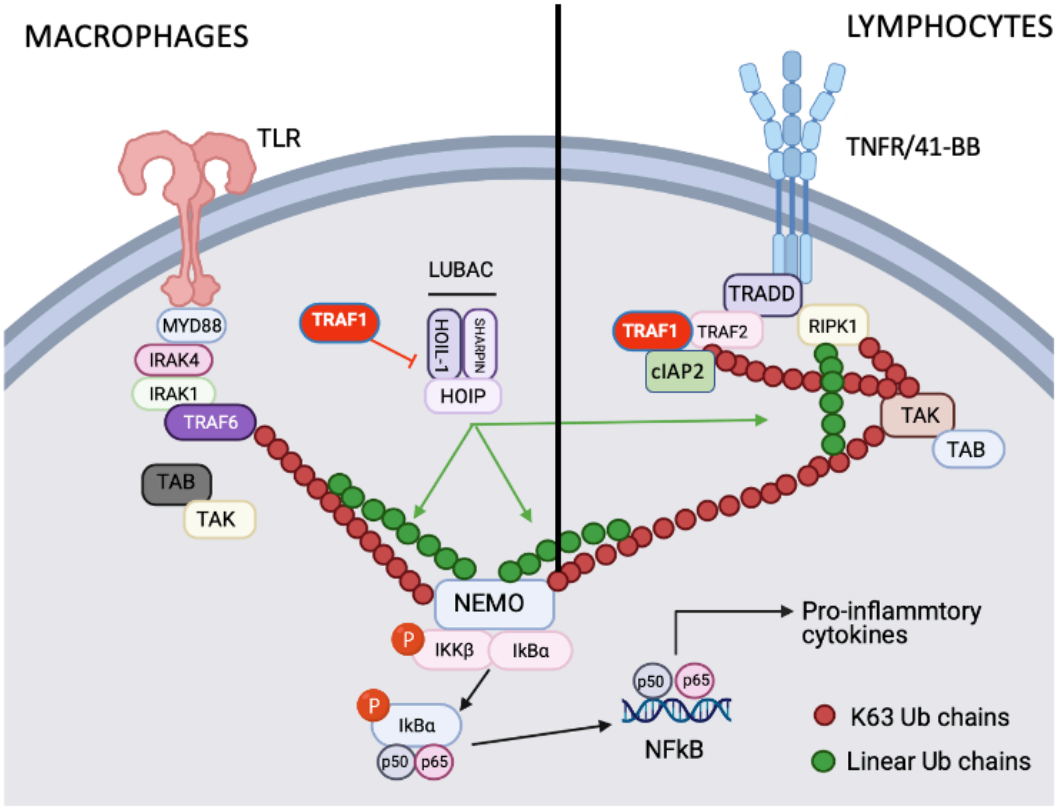

Figure 19 Summary of the multifaceted TRAF1 protein downstream of innate and adaptive immune system. Image created on BioRender.com.

6.0 FUTURE DIRECTIONS

This thesis successfully identified residues within the mTRAF1 protein that are responsible for the NF-κB activation cascade downstream of the innate and adaptive immune systems. The next step is to create a knock-in mouse would that have these mutated versions of mTRAF1 which would allow us to examine their effects on the state of inflammation within this model. This will allow us to examine the direct role of TRAF1 and its implications in the pathology of genetically induced RA. In addition, this will allow for a greater understanding of this pathology, possibly leading to the development of targeted therapies for this chronic inflammatory disease.

With the insights of this study, the residues that have been found to be responsible for TRAF1 interactions in TLRs and TNFRs, will allow us to isolate the many roles of TRAF1 in either pathway. Essentially, incorporating these mutations into a mouse model will allow us to examine how inflammation is affected when the interaction between mTRAF1: mcIAP2 is abrogated. We believe the dissociation of these 2 proteins will lead to decreased proliferation and survival of T lymphocytes ultimately leading to reduced inflammation.

REFERNCES

1. Feldmann, M., F. M. Brennan, and R. N. Maini. 1996. Role of Cytokines in Rheumatoid Arthritis. *Annu. Rev. Immunol.* 14: 397–440.

2. McInnes, I. B., and G. Schett. 2007. Cytokines in the pathogenesis of rheumatoid arthritis. *Nat. Rev. Immunol.* 7: 429–442.

3. Firestein, G. S. 2003. Evolving concepts of rheumatoid arthritis. *Nature* 423: 356–361.

4. Okada, Y., S. Eyre, A. Suzuki, Y. Kochi, and K. Yamamoto. 2019. Genetics of rheumatoid arthritis: 2018 status. *Ann. Rheum. Dis.* 78: 446–453.

5. Silman, A. J., and J. E. Pearson. 2002. Epidemiology and genetics of rheumatoid arthritis. *Arthritis Res.* 4 Suppl 3: S265-272.

6. Nishimura, K., D. Sugiyama, Y. Kogata, G. Tsuji, T. Nakazawa, S. Kawano, K. Saigo, A. Morinobu, M. Koshiba, K. M. Kuntz, I. Kamae, and S. Kumagai. 2007. Meta-analysis: diagnostic accuracy of anti-cyclic citrullinated peptide antibody and rheumatoid factor for rheumatoid arthritis. *Ann. Intern. Med.* 146: 797–808.

7. Feldmann, M., and R. N. Maini. 2002. Discovery of TNF-alpha as a therapeutic target in rheumatoid arthritis: preclinical and clinical studies. *Joint Bone Spine* 69: 12–18.

8. Abdul-Sater, A. A., M. I. Edilova, D. L. Clouthier, A. Mbanwi, E. Kremmer, and T. H. Watts. 2017. The signaling adaptor TRAF1 negatively regulates Toll-like receptor signaling and this underlies its role in rheumatic disease. *Nat. Immunol.* 18: 26–35.

9. Takeda, K., and S. Akira. 2005. Toll-like receptors in innate immunity. *Int. Immunol.* 17: 1–14.

10. Verstrepen, L., T. Bekaert, T.-L. Chau, J. Tavernier, A. Chariot, and R. Beyaert. 2008. TLR-4, IL-1R and TNF-R signaling to NF-κB: variations on a common theme. *Cell. Mol. Life Sci.* 65: 2964–2978.

11. Yang, Y., R. Feng, Y.-Z. Wang, H.-W. Sun, Q.-M. Zou, and H.-B. Li. 2020. Toll-like receptors: Triggers of regulated cell death and promising targets for cancer therapy. *Immunol. Lett.* 223: 1–9.

12. Akira, S. 2003. Toll-like Receptor Signaling. *J. Biol. Chem.* 278: 38105–38108.

13. Dhillon, B., F. Aleithan, Z. Abdul-Sater, and A. A. Abdul-Sater. 2019. The Evolving Role of TRAFs in Mediating Inflammatory Responses. *Front. Immunol.* 10.

14. Oeckinghaus, A., and S. Ghosh. 2009. The NF-κB Family of Transcription Factors and Its Regulation. *Cold Spring Harb. Perspect. Biol.* 1: a000034.

15. Zhou, H., I. Wertz, K. O'Rourke, M. Ultsch, S. Seshagiri, M. Eby, W. Xiao, and V. M. Dixit. 2004. Bcl10 activates the NF-κB pathway through ubiquitination of NEMO. *Nature* 427: 167–171.

16. Adli, M., E. Merkhofer, P. Cogswell, and A. S. Baldwin. 2010. IKKα and IKKβ Each Function to Regulate NF-κB Activation in the TNF-Induced/Canonical Pathway. *PLoS ONE* 5: e9428.

17. 1995. *Advances in Immunology*,. Academic Press.

18. Shih, V. F.-S., R. Tsui, A. Caldwell, and A. Hoffmann. 2011. A single NFκB system for both canonical and non-canonical signaling. *Cell Res.* 21: 86–102.

19. Sun, S.-C. 2011. Non-canonical NF-κB signaling pathway. *Cell Res.* 21: 71–85.

20. Fujita, H., S. Rahighi, M. Akita, R. Kato, Y. Sasaki, S. Wakatsuki, and K. Iwai. 2014. Mechanism Underlying IκB Kinase Activation Mediated by the Linear Ubiquitin Chain Assembly Complex. *Mol. Cell. Biol.* 34: 1322–1335.

21. Varshavsky, A. 1997. The ubiquitin system. *Trends Biochem. Sci.* 22: 383–387.

22. Rittinger, K., and F. Ikeda. 2017. Linear ubiquitin chains: enzymes, mechanisms and biology. *Open Biol.* 7.

23. Haas, T. L., C. H. Emmerich, B. Gerlach, A. C. Schmukle, S. M. Cordier, E. Rieser, R. Feltham, J. Vince, U. Warnken, T. Wenger, R. Koschny, D. Komander, J. Silke, and H. Walczak. 2009. Recruitment of the linear ubiquitin chain assembly complex stabilizes the TNF-R1 signaling complex and is required for TNF-mediated gene induction. *Mol. Cell* 36: 831–844.

24. Tokunaga, F., T. Nakagawa, M. Nakahara, Y. Saeki, M. Taniguchi, S. Sakata, K. Tanaka, H. Nakano, and K. Iwai. 2011. SHARPIN is a component of the NF-κB-activating linear ubiquitin chain assembly complex. *Nature* 471: 633–636.

25. Walczak, H., K. Iwai, and I. Dikic. 2012. Generation and physiological roles of linear ubiquitin chains. *BMC Biol.* 10: 23.

26. Liu, T., L. Zhang, D. Joo, and S.-C. Sun. 2017. NF-κB signaling in inflammation. *Signal Transduct. Target. Ther.* 2: 17023.

27. So, T., and N. Ishii. 2019. The TNF-TNFR Family of Co-signal Molecules. *Adv. Exp. Med. Biol.* 1189: 53–84.

28. Quistad, S. D., and N. Traylor-Knowles. 2016. Precambrian origins of the TNFR superfamily. *Cell Death Discov.* 2: 16058.

29. Dempsey, P. W., S. E. Doyle, J. Q. He, and G. Cheng. 2003. The signaling adaptors and pathways activated by TNF superfamily. *Cytokine Growth Factor Rev.* 14: 193–209.

30. Wajant, H., F. Henkler, and P. Scheurich. 2001. The TNF-receptor-associated factor family: scaffold molecules for cytokine receptors, kinases and their regulators. *Cell. Signal.* 13: 389–400.

31. Lalani, A. I., S. Zhu, S. Gokhale, J. Jin, and P. Xie. 2018. TRAF molecules in inflammation and inflammatory diseases. *Curr. Pharmacol. Rep.* 4: 64–90.

32. Xie, P. 2013. TRAF molecules in cell signaling and in human diseases. *J. Mol. Signal.* 8: 7.

33. Chung, J. Y., Y. C. Park, H. Ye, and H. Wu. 2002. All TRAFs are not created equal: common and distinct molecular mechanisms of TRAF-mediated signal transduction. *J. Cell Sci.* 115: 679–688.

34. McPherson, A. J., L. M. Snell, T. W. Mak, and T. H. Watts. 2012. Opposing Roles for TRAF1 in the Alternative versus Classical NF-κB Pathway in T Cells. *J. Biol. Chem.* 287: 23010–23019.

35. Vinay, D. S., and B. S. Kwon. 2011. 4-1BB signaling beyond T cells. *Cell. Mol. Immunol.* 8: 281–284.

36. Zheng, C., V. Kabaleeswaran, Y. Wang, G. Cheng, and H. Wu. 2010. Crystal Structures of the TRAF2: cIAP2 and the TRAF1: TRAF2: cIAP2 Complexes: Affinity, Specificity, and Regulation. *Mol. Cell* 38: 101–113.

37. Vince, J. E., D. Pantaki, R. Feltham, P. D. Mace, S. M. Cordier, A. C. Schmukle, A. J. Davidson, B. A. Callus, W. W.-L. Wong, I. E. Gentle, H. Carter, E. F. Lee, H. Walczak, C. L. Day, D. L. Vaux, and J. Silke. 2009. TRAF2 Must Bind to Cellular Inhibitors of Apoptosis for Tumor Necrosis Factor (TNF) to Efficiently Activate NF-κB and to Prevent TNF-induced Apoptosis. *J. Biol. Chem.* 284: 35906–35915.

38. Vaux, D. L., and J. Silke. 2005. IAPs, RINGs and ubiquitylation. *Nat. Rev. Mol. Cell Biol.* 6: 287–297.

39. Li, X., Y. Yang, and J. D. Ashwell. 2002. TNF-RII and c-IAP1 mediate ubiquitination and degradation of TRAF2. *Nature* 416: 345–347.

40. Gyrd-Hansen, M., and P. Meier. 2010. IAPs: from caspase inhibitors to modulators of NF-κB, inflammation and cancer. *Nat. Rev. Cancer* 10: 561–574.

41. Cheng, T., Y. Choi, T. H. Finkel, P. Y. Tsao, M. Q. Ji, and R. A. Eisenberg. 2013. Tumor Necrosis Factor Receptor-associated Factor 1 influences KRN/I-Ag7 Mouse Arthritis Autoantibody Production. *J. Clin. Immunol.* 33: 759–766.

42. Kim, C. M., J. Y. Choi, E. A. Bhat, J.-H. Jeong, Y.-J. Son, S. Kim, and H. H. Park. 2016. Crystal structure of TRAF1 TRAF domain and its implications in the TRAF1-mediated intracellular signaling pathway. *Sci. Rep.* 6: 25526.

APPENDIX A

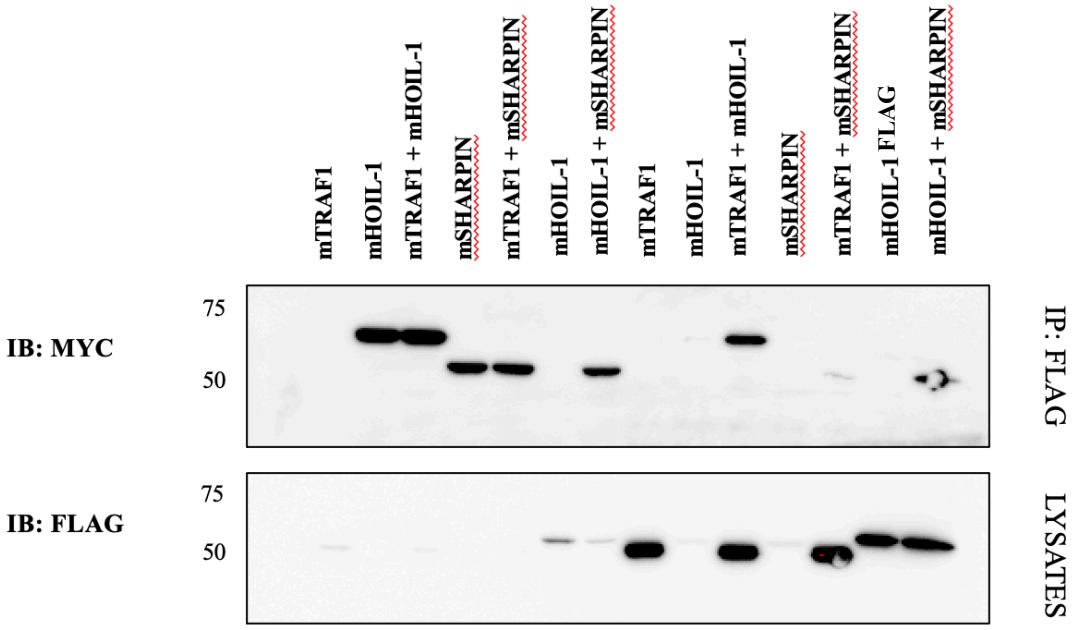

Figure 7 interaction between mTRAF1 and mLUBAC and mLUBAC components, mHOIL-1 and mSHARPIN. Co-immunoprecipitation of mTRAF1 lysates of HEK293T/17 cells, followed by immunoblotting (IB) with Myc and Flag specific antibodies and light-chain-specific anti-Rabbit-horseradish perioxidase and anti-mouse.

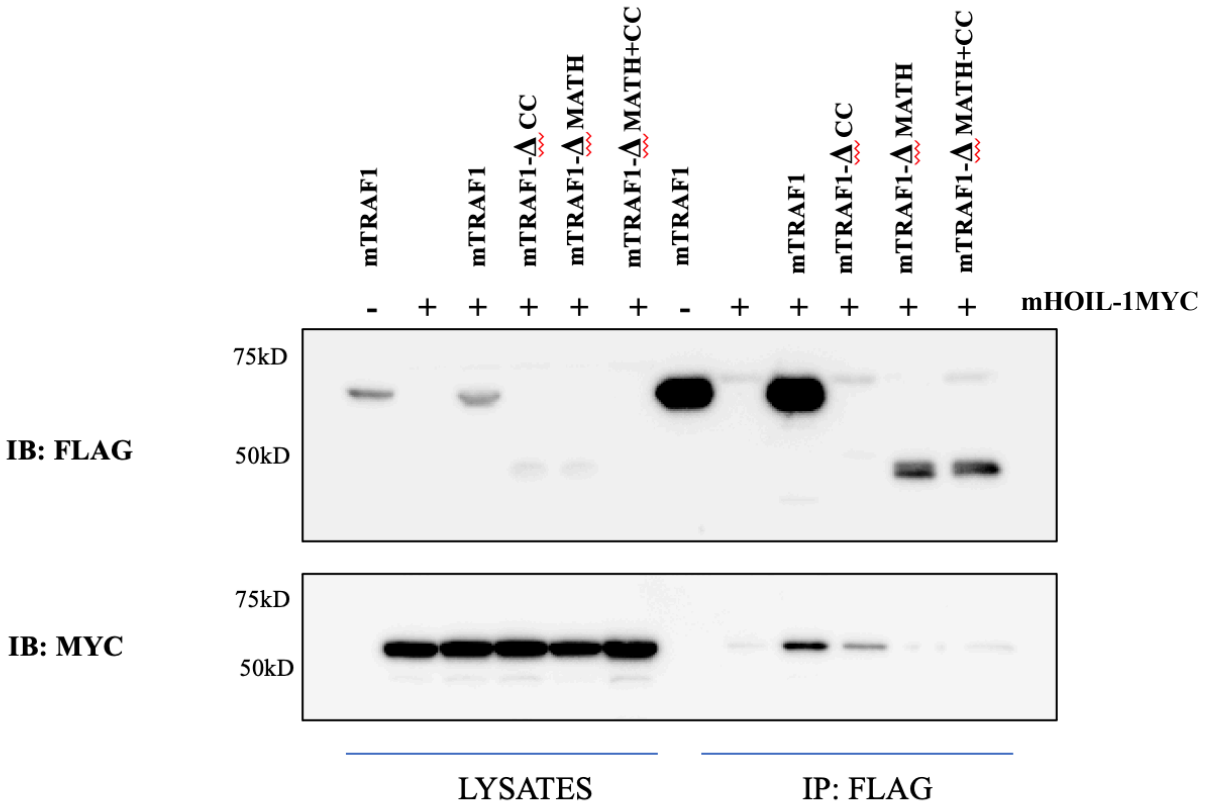

Figure 8 effects of mTRAF1 deletions on mHOIL-1. Co-immunoprecipitation of mTRAF1 lysates of HEK293T/17 cells, followed by immunoblotting (IB) with Myc and Flag specific antibodies and light-chain-specific anti-Rabbit- and light-chain-specific anti-mouse. This experiment was conducted three independent times.

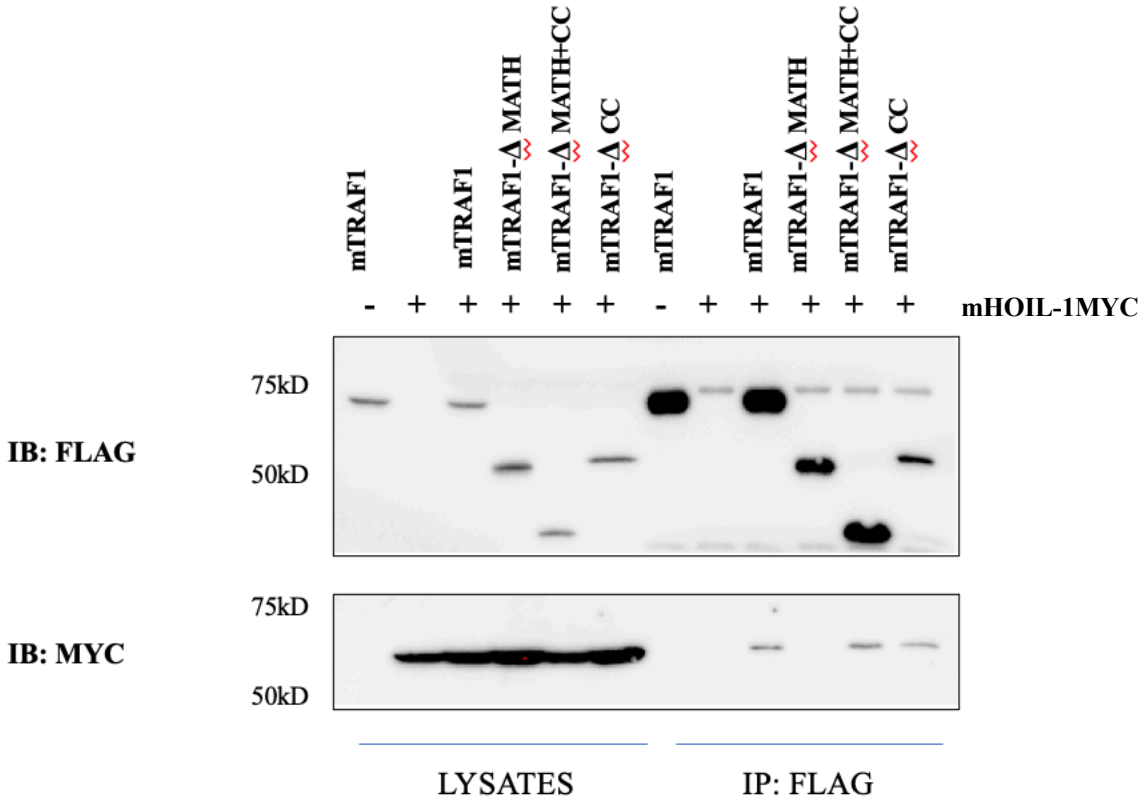

Figure 9. Effects of mTRAF1 deletions on mHOIL-1. Co-immunoprecipitation of mTRAF1 lysates of HEK293T/17 cells, followed by immunoblotting (IB) with Myc and Flag specific antibodies and light-chain-specific anti-Rabbit- and light-chain-specific anti-mouse.

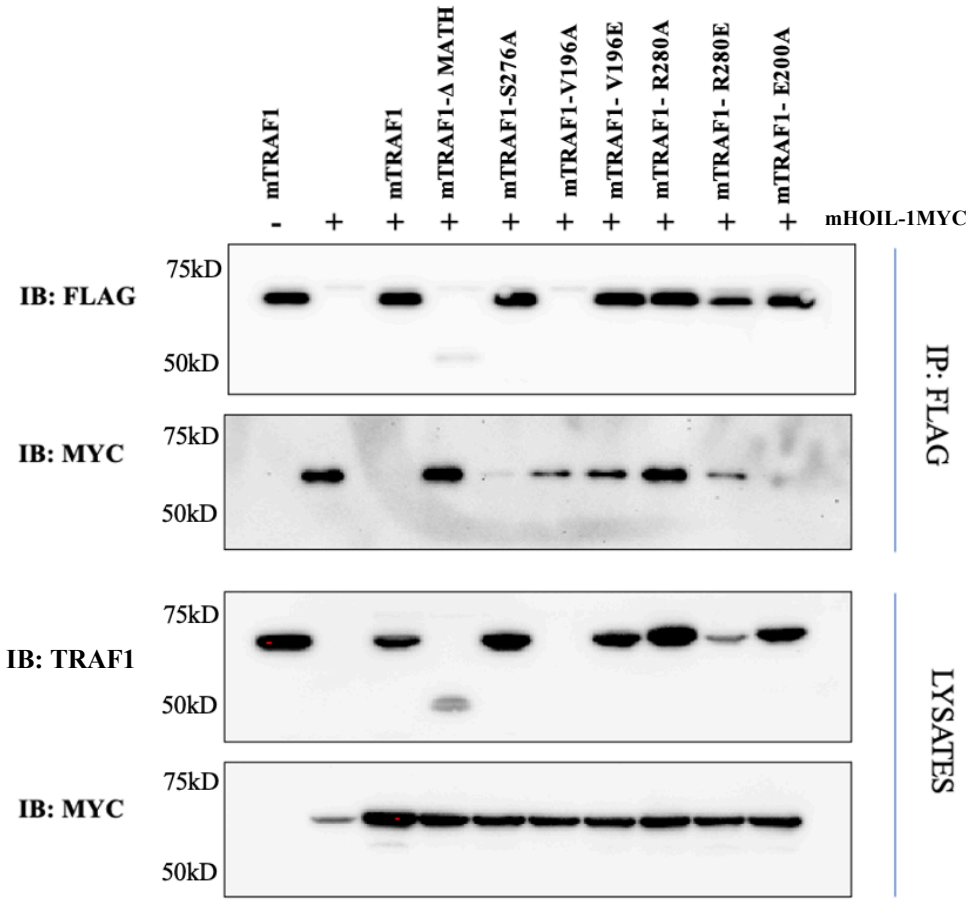

Figure 10 effects of single mTRAF1 mutations on mHOIL-1. Co-immunoprecipitation of mTRAF1 lysates of HEK293T/17 cells, followed by immunoblotting (IB) with Myc and Flag specific antibodies and light-chain-specific anti-Rabbit- and light-chain-specific anti-mouse. This experiment was conducted three independent times.

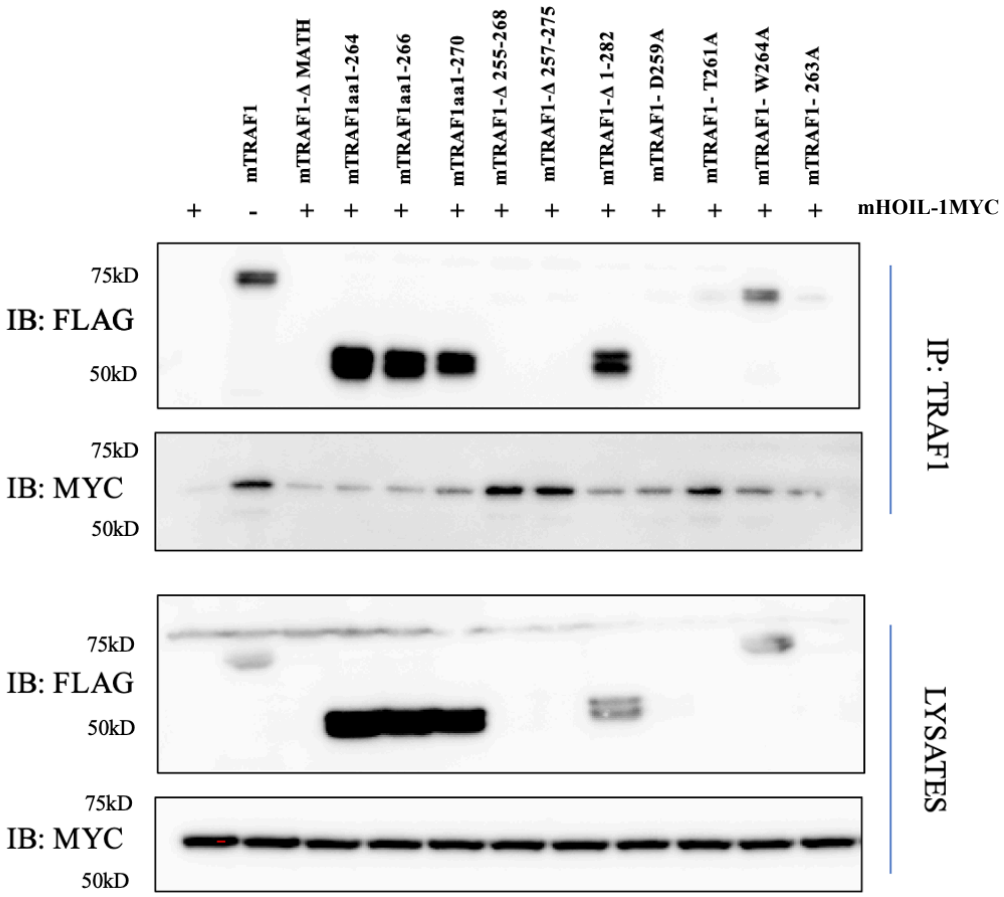

Figure 11 effects of mTRAF1 mutations/truncations on mHOIL-1. Co-immunoprecipitation of mTRAF1 lysates of HEK293T/17 cells, followed by immunoblotting (IB) with Myc and Flag specific antibodies and light-chain-specific anti-Rabbit- and light-chain-specific anti-mouse. This experiment was conducted three independent times.

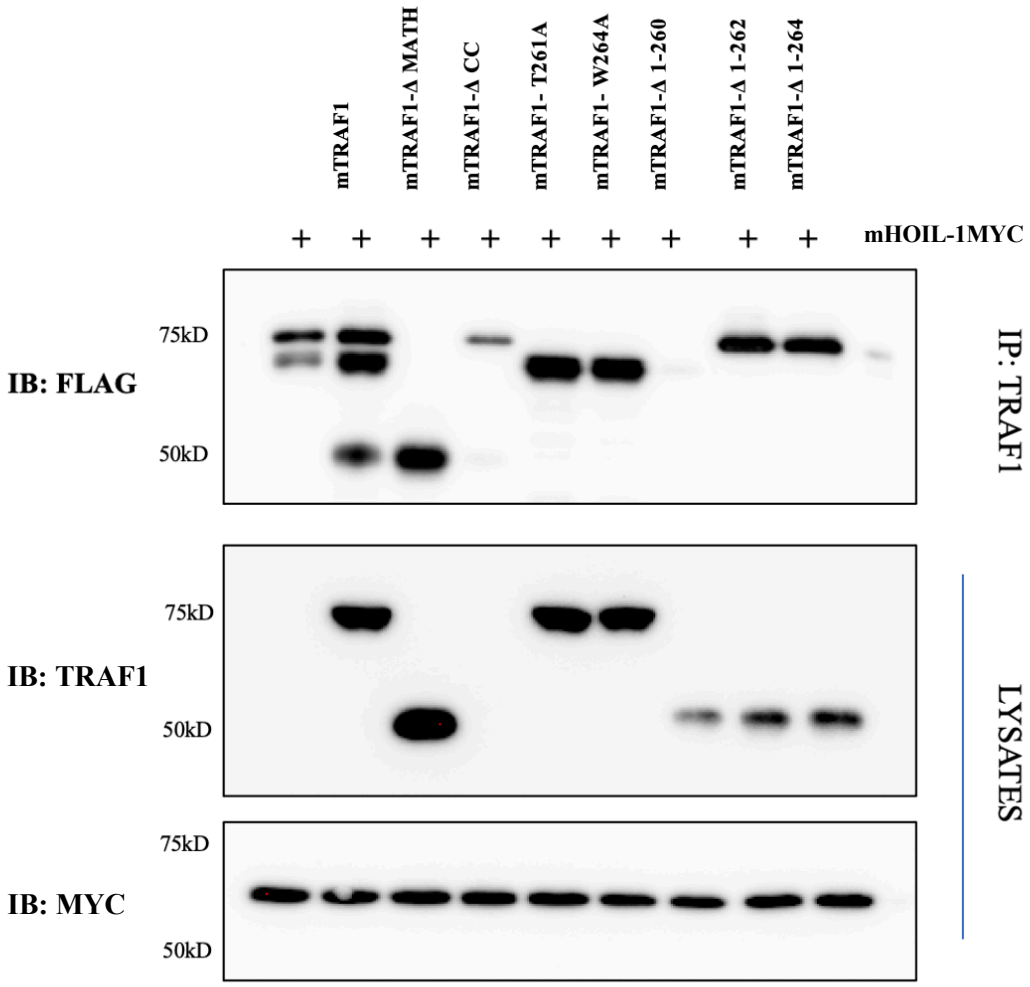

Figure 12 effects of mTRAF1 truncations/mutations on mHOIL-1. Co-immunoprecipitation of mTRAF1 lysates of HEK293T/17 cells, followed by immunoblotting (IB) with Myc and Flag specific antibodies and light-chain-specific anti-Rabbit- and light-chain-specific anti-mouse. This experiment was conducted three independent times.

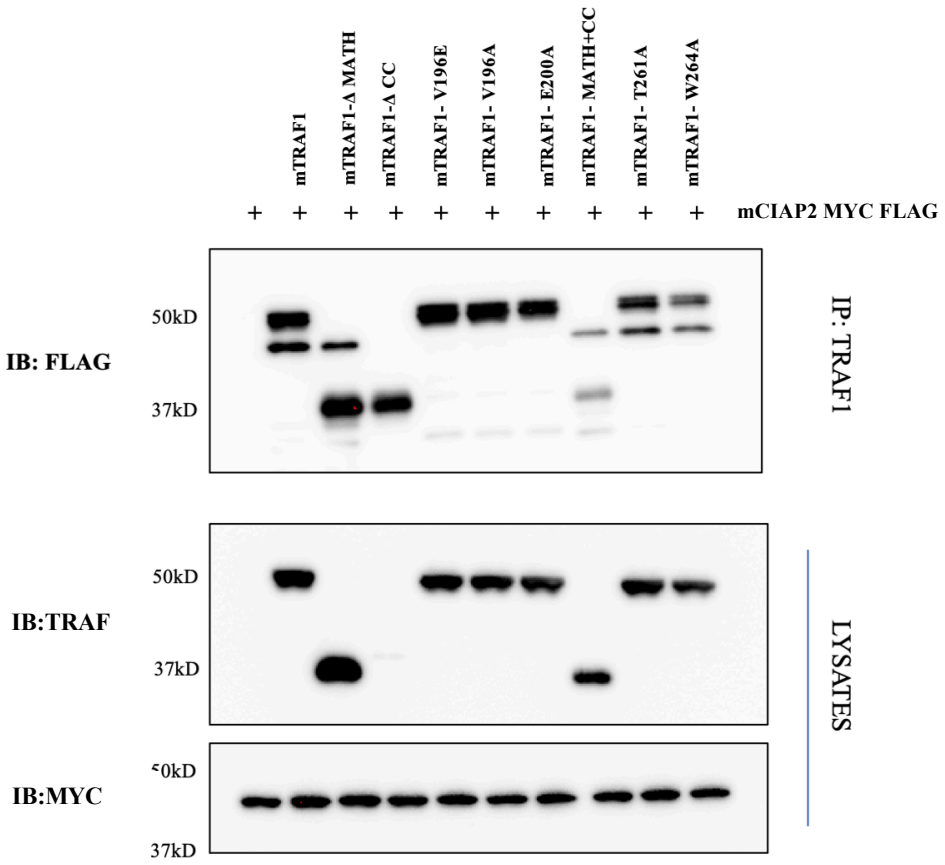

Figure 13 effects of single mTRAF1 deletions/mutations on mcIAP2. Co-immunoprecipitation of mTRAF1 lysates of HEK293T/17 cells, followed by immunoblotting (IB) with Myc and Flag specific antibodies and light-chain-specific anti-Rabbit- and light-chain-specific anti-mouse. This experiment was conducted three independent times.

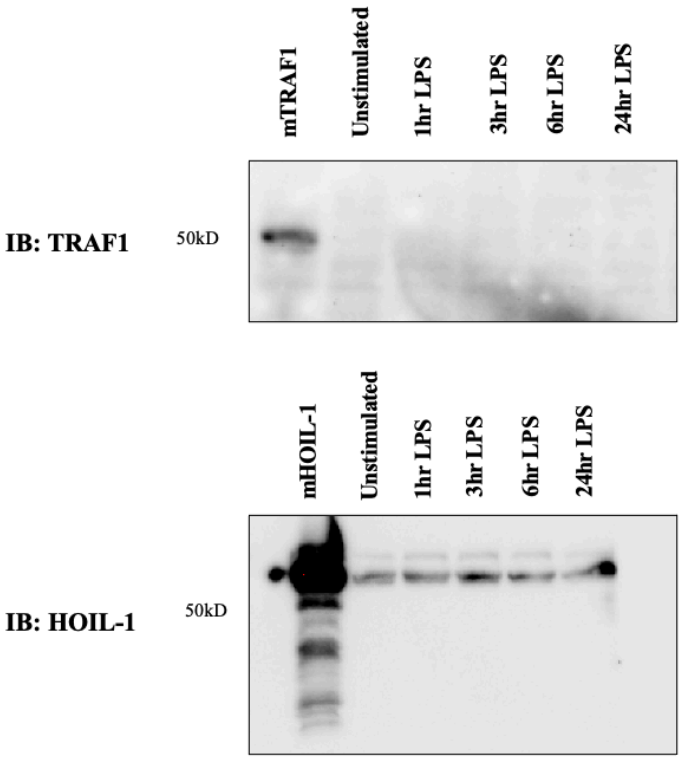

Figure 14 Effects of LPS stimulations in Raw 264.7 cells at various time points. Cell lysates of Raw 264.7 cells stimulated with 100ng/ml of LPS at 0 hr, 1 hr, 3hr, 6 hr, and 24 hr. Immunoblotting with TRAF1 and HOIL-1 specific antibodies and light-chain-specific anti-Rabbit- and light-chain-specific anti-mouse.